Identifying the genetic determinants of lipophagy in *Saccharomyces cerevisiae*

Garrett Fairman

Thesis submitted to the University of Ottawa
in partial fulfillment of the requirements for the
MSc. degree in Biochemistry

Department of Biochemistry, Microbiology, and Immunology
Faculty of Medicine
University of Ottawa

Abstract

Lipid droplet (LD) autophagy (lipophagy) is a recently discovered selective form of autophagy and is a pathway for LD catabolism through the lysosome or vacuole. Therefore, lipophagy has therapeutic potential in the treatment of a variety of lipid related diseases in which increased cellular LDs are associated with pathophysiologies, such as obesity or atherosclerosis. This ubiquitous process has been an ongoing area of research within the budding yeast, *Saccharomyces cerevisiae*. However, there remains a need to better understand the regulators of this process. I have developed and validated a lipophagy library in yeast for the assessment of novel genetic regulators of stationary phase induced lipophagy. Through the screening of my library for roles in lipophagy I have identified many genetic regulators of lipophagy which include *CUE1, UBC7, LHS1, HSP31, PLN1, TFS1, LAM6, OSH3, OSH4* and *OSH7*, among others. My screen highlights the power of this library to identify lipophagy regulators in *S. cerevisiae*, which can be utilised in the future to further the understanding of lipophagy.

Abbreviations

CMA	Chaperone mediated autophagy
ER	Endoplasmic reticulum
LD	Lipid droplet
LDL	Low-density lipoprotein
SD-N	Nitrogen starvation
L_o microdomain	Liquid-ordered microdomain
L_d microdomain	Liquid-disordered microdomain
EGO-TC	Ego1-Ego2-Ego3 ternary complex
ATG	Autophagy related gene
PAS	Phagophore assembly site
PE	Phosphatidylethanolamine
GUV	Giant unilamellar vesicle
NPC	Niemann Pick type C
PtdIns	Phosphatidylinositol
PtdIns(4)P	Phosphatidylinositol-4 phosphate
PtdIns(3)P	Phosphatidylinositol-3 phosphate
NVJ	Nuclear vacuole junction
OSH	Oxysterol binding protein homolog
OSBP	Oxysterol binding protein
ORD	OSBP-related domain
PH	Pleckstrin homology
ORP	OSBP-related protein
PS	Phosphatidylserine
Hyg	Hygromycin
Nat	Nourseothricin
DMA	Deletion mutant array
SC	Synthetic complete
SD	Synthetic dropout
OA	Oleic acid
SGA	Synthetic genetic array
MDH	Monodansylpentane
CMAC	7-amino-4-chloromethylcoumarin
GPCR	G-protein coupled receptor
PtdIns(3)-K	Phosphatidylinositol-3 kinase
ERAD	Endoplasmic reticulum associated degradation
TM	Tunicamycin
DTT	Dithiothreitol
AMPK	AMP-activated protein kinase
TRAPP	Transport protein particle
RTG	Retrograde pathway
TRPML	Transient receptor potential-mucolipin
LAM	Lipid transfer proteins anchored at membrane contact sites
StART	Steroidogenic acute regulatory transfer
BAR	Bin/Amphiphysin/Rvs167

IB	Inclusion body

List of Figures

List of Tables

Table of Contents

1.0 Introduction

1.1 Types of autophagy

Autophagy is a cellular process in which organelles, proteins or other macromolecules undergo lysosomal or vacuolar degradation and nutrients released from these cargoes are recycled[1]. Lysosomes are acidic organelles containing hydrolytic enzymes. Some organisms, like budding yeast, instead have a lytic vacuole that has the same function in autophagy[1,2]. Autophagy is important for the maintenance of cellular homeostasis through the removal of damaged organelles and misfolded proteins, the generation of nutrients in starvation conditions and overall cellular metabolism[1]. Autophagy is broadly defined into three subtypes: macro, micro and chaperone-mediated autophagy (CMA). In macroautophagy, cargo is sequestered by a double-membraned autophagosome that subsequently fuses with a lysosome/vacuole for degradation[3]. Microautophagy refers to the internalization of cargo by the lysosome/vacuole for degradation in the absence of autophagosome sequestration of cargo[4]. In CMA, proteins bearing the KFERQ pentapeptide sequence are recognized then degraded by the lysosome[5]. The processes of Macro- and microautophagy have been found to occur selectively and in-bulk in a variety of organisms[4,6]. Bulk autophagy is general and does not discriminate in cargo choice, whereas selective forms of these autophagies predominantly target a specific type of cargo[1,4]. Some examples of selective autophagy include mitophagy, ERphagy and lipophagy, which selectively degrade mitochondria, endoplasmic reticulum (ER) and lipid droplets (LDs), respectively. LDs and lipophagy are the focus of the work discussed herein.

1.2 Lipid droplets, lipophagy and potential applications

LDs are a ubiquitous energy-rich organelles that originate from the ER and act as storage sites of cellular lipids[7–9]. Comprised of a neutral lipid core of triacylglycerols and steryl esters, LDs are

surrounded by a phospholipid monolayer that is associated with proteins that regulate LD metabolism[7–9]. LDs are important for cellular energy production, phospholipid biosynthesis, act as sources of precursors for bioactive lipid signaling molecules – like eicosanoids, and are involved in overall lipid homeostasis[7–10]. They also prevent lipotoxicity through the storage of excess lipids and assist in ER homeostasis[9]. As LD biology continues to be explored, it is becoming increasingly clear that these organelles are connected to a variety of diseases[7–9]. Obesity and atherosclerosis are two highly relevant diseases in western society that LDs are involved in the pathophysiology of[7–9]. In obesity, an accumulation of lipid overwhelms the adipose tissue capacity to store LDs[11]. The resulting excess lipid deposition in adipose and non-adipose tissue leads to lipotoxicity and downstream complications such as steatosis, insulin resistance and chronic inflammation[7,9,11]. Atherosclerosis is characterized by the development of arterial plaques that can lead to ischemic events. In this disease, macrophages, and vascular smooth cells in the subendothelial layer of the vascular become LD laden foam cells following excessive uptake of cholesterol rich low-density lipoprotein (LDL)[8]. The lipid burden of foam cells leads to activation of pro-inflammatory signaling and increased apoptosis, among other metabolic dysregulations, that contribute to the progression and severity of atherosclerotic plaques[8,12]. Given the role of LDs in metabolic disease, there is a great importance and therapeutic potential in understanding the mechanisms behind LD catabolism. Lipophagy is a recently described selective form of autophagy in which LDs are the cargo degraded by lysosomes or lytic vacuoles[13]. This seemingly ubiquitous process has been observed across a variety of organisms including several mammalian cell types[13,14], flies (*drosophila*)[15], plants[16], and lower-order eukaryotes like budding yeast, *Saccharomyces cerevisiae*[17], which is the focus of this thesis. However, there are notable mechanistic differences for lipophagy across different organisms, as well as across the distinct modes of lipophagy

induction within a given organism. Investigations into mammalian hepatocytes and macrophages reveal that lipophagy can operate through a macroautophagic mechanism, as shown by localizations of LDs with LC3 labelled double-membranes, described as autophagosomes, and impairments in LD catabolism in macrophages where genes of the core macroautophagy machinery are inhibited[13,14]. Additionally, there is an emerging body of evidence to support that microautophagic forms of lipophagy, in which LDs become internalized by degradative lysosomes in the absence of autophagosome sequestration, are also present in these same cell types[18–20]. Lipophagy in *S. cerevisiae* solely operates through a microautophagic-like mechanism. whereby LDs are directly taken up via the vacuole[17,21–25]. In most cases however, macroautophagy components are also required for yeast lipophagy to ensue[17,21,22,26]. *S. cerevisiae* has proven to be a versatile organism for the study of autophagy over the past several decades, and this remains true for lipophagy. Microlipophagy has been experimentally induced in yeast through nutrient starvation or cell stress[17,21,22,24,25,27–29]. The two induction methodologies that will form the basis of this work are nitrogen starvation (SD-N) and stationary phase growth[17,22,23,26].

1.3 Modes of yeast lipophagy induction

SD-N is a type of nutrient starvation that activates autophagy and is induced with media depleted of amino acids and ammonium sulfate[17,23]. During stationary phase growth cells divide rapidly in a nutrient rich media until they deplete the glucose via glycolysis, at which point they will undergo diauxic shift, slowing proliferation and switching to aerobic respiration[22,30]. As is relevant for lipophagy, LDs also proliferate in these conditions of nutrient depletion[31]. Eventually, the stationary phase is entered where cell division is halted, and survival pathways become activated to combat starvation[22,30]. It has been shown that lipophagy becomes maximally active at

approximately the fifth day of stationary phase[22], which is the growth time I used throughout this work when measuring stationary phase induced lipophagy. There are two other primary methodologies used in the literature to induce lipophagy: acute glucose reduction[21,32], and ER stress/lipid stress[24,25,27]. While these are not focused on in my study, the relevant findings from these works will be explored in the context of my observations.

1.4 Overview of microlipophagy in *S. cerevisiae*

Depending on the mode of induction, lipophagy in budding yeast has a unique set of genetic requirements. Table 1 summarizes the current knowledge base of yeast lipophagy regulators as well as highlights some of these differences in lipophagy variants. It is important to note that genes involved in lipophagy have not all been tested for each induction mode. Therefore, additional commonalities or differences between each lipophagy process may yet be uncovered. For each modality, lipophagy is facilitated by the formation of vacuolar liquid-ordered (L_o) microdomains[21–23,27,33] (Figure 1). L_o microdomains are distinct lipid-raft regions with high concentrations of membrane sterol lying in contrast to L_d (liquid-disordered) microdomains[33]. Both L_o and L_d microdomains have distinct lipid and protein profiles that confer specific functionalities[22,33]. Some of the proteins that segregate to the L_d domain include Vph1, a vacuolar ATPase subunit, and Ncr1, a sterol transporter, among other proteins containing multiple transmembrane helices, while proteins that segregate to the L_o domain include Ivy1, and Gtr2, proteins that interact with the Ego1-Ego2-Ego3 ternary complex (EGO-TC) – an amino acid sensor that regulates cell growth and microautophagy[33–37]. This complex will be discussed further in Chapter 4.1. As yeast are placed under continued stress, the complexity of the microdomain pattern evolves[22]. For example, prolonged growth into the late stationary phase, increases the number of microdomains and their appearance changes from sheet-like to a complex reticular lattice[22,33]. In

lipophagy stimulating conditions, LDs interact with the L_o microdomains, altering membrane curvature and allowing for inwards budding of vacuolar membrane into the vacuolar lumen for LD internalization[22,23]. In agreement with this, a recent study highlights that yeast depleted of phosphate are defective in lipophagy, possibly due to an impairment in vacuolar microdomain formation as these cells have low levels of free ergosterol, a key component of L_o microdomains[38]. Most forms of yeast lipophagy require the core autophagy (*ATG)* genes (Table 1), indicating that macroautophagy is indispensable, even though phenotypically lipophagy in yeast resembles microautophagy. Some notable overlapping ATG requirements between lipophagy induced by stationary phase and SD-N include: Atg1 – a kinase required for the activation of autophagy. This kinase has roles in recruiting autophagy factors like Atg9 positive vesicles to the phagophore assembly site (PAS) for early autophagosome formation[39], Atg8 – a factor conjugated to phosphatidylethanolamine (PE) that is required for autophagosome expansion[3,40], Atg7 – a component of the complex that conjugates Atg8 to PE[3,40], and Atg15 – a vacuolar lipase[41]. It is unclear why most forms of yeast microlipophagy also require general macroautophagy. However, early work into the lipid-raft like microdomains may offer an answer. These domains were first assessed in giant unilamellar vesicles (GUVs) where the membrane partitioning was also dependent on sphingolipid species with saturated acyl chains that were proposed to tightly pack together with sterol[33,42]. This observation may be true for the yeast vacuole as well, given the intimacy of sphingolipid metabolism and vacuolar homeostasis[43]. Therefore, one possibility for the requirement of macroautophagy and the *ATG* genes required in most microlipophagy variants is to provide membrane sphingolipids for microdomain formation via autophagosome-vacuole fusion[23,44]. However, the incorporation of other membrane lipids with saturated acyl chains into the vacuole is also a possibility.

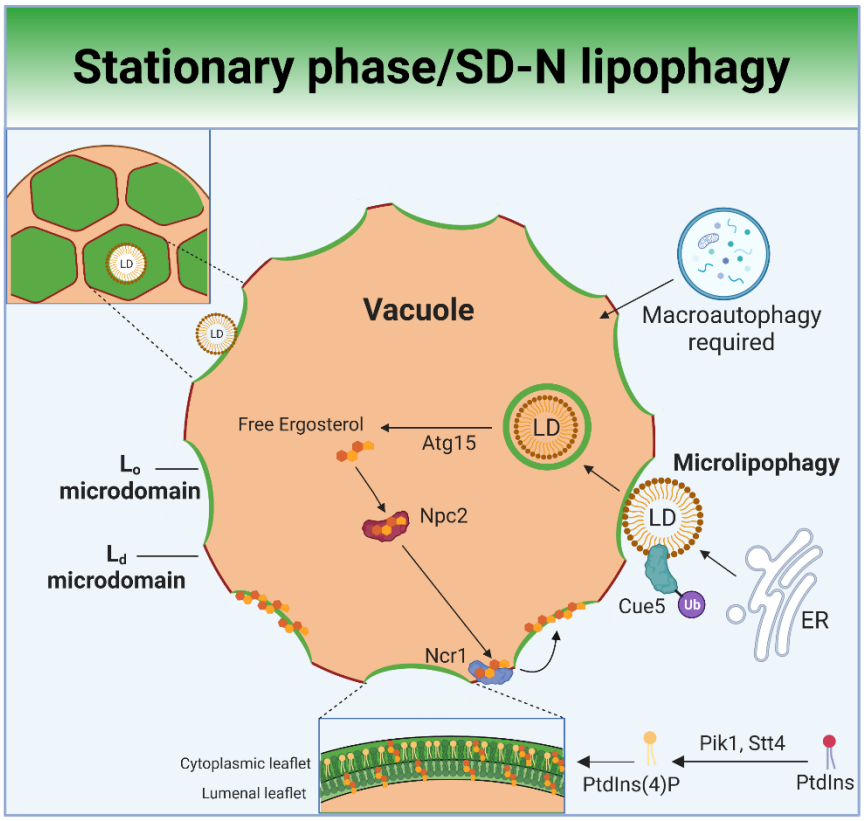

Figure 1. Overview of known stationary phase/SD-N induced lipophagy mechanism in yeast.

1.5 Summary of select known regulators of yeast lipophagy induced by stationary phase and nitrogen starvation

The formation of vacuolar L_o microdomains for lipophagy induced by stationary phase and SD-N induced requires Ncr1 and Npc2, homologs of mammalian Niemann Pick Type C (NPC) genes 1 and 2, respectively[23]. Ncr1 and Npc2, found in the vacuolar membrane and lumen respectively during stationary phase growth, help traffic and incorporate sterol into the vacuolar membrane to form and expand L_o microdomains (Figure 1)[23]. Structural analysis shows that vacuolar sterol is transferred from a hydrophobic pocket within Npc2 to the N-terminal domain of Ncr1 where it travels through a tunnel within Ncr1 for insertion into the vacuolar membrane[45]. Intriguingly, deletion of *NPC2* leads to greater impairment in lipophagy than deletion of *NCR1* during lipophagy induced by stationary phase and SD-N[23]. This, coupled with the finding that Npc2 and Ncr1 work in conjunction to traffic vacuolar sterol for L_o microdomain formation and expansion, raise the question as to whether Npc2 may also interact with other proteins to traffic sterol? Additionally, vacuolar microdomains are not completely abolished in NPC deletion yeast[23]. This suggests a role for additional cell components in this process. The identities of other proteins that might facilitate vacuolar membrane sterol insertion are currently under investigation. One possibility is that phosphatidylinositol 4-kinases, which are involved in the formation of phosphatidylinositol 4-phosphate (PtdIns(4)P), might facilitate vacuolar membrane sterol insertion. Two of these kinases in yeast, Pik1 and Stt4, but not Lsb6, play roles in lipophagy induced by both stationary phase and SD-N[46]. Under these conditions, Pik1 and Stt4 are required for the proper localization of PtdIns(4)Ps to the cytoplasmic leaflet of L_o vacuolar microdomains and of microautophagic vesicles, as well as the proper formation of microautophagic vesicles[46]. Given these findings and other observations that LDs interact at PtdIns(4)P-rich L_o vacuolar microdomains, one hypothesis

is that lipid exchange of ergosterol for PtdIns(4)P can occur between LDs and the cytoplasmic leaflet of the vacuolar membrane to aid in microdomain maintenance[46,47]. Lam6, a protein highly concentrated at the nuclear vacuole junction (NVJ) is also capable of sterol transport and has been shown to transfer ergosterol to the vacuolar membrane, and play a role in vacuolar microdomain formation[48]. However, Lam6 involvement in vacuolar microdomain formation was not assessed for stationary phase growth conditions[48]. It remains an open question if other non-vesicular lipid transport proteins in yeast are involved in lipophagy as well. Following vacuolar internalization of LDs, the vacuolar lipase Atg15, which also degrades autophagic bodies, is required to mobilize neutral lipids from LDs[17]. Atg15 is involved in lipophagy induced by SD-N[17] and stationary phase[22]. Intriguingly, stationary phase-induced lipophagy shows an impairment in LD-vacuolar entry following *ATG15* deletion[22]. This is possibly due to impaired L_o microdomain formation because of the reduced ability to liberate LD sterol. Loss of the ability of Atg15 to degrade autophagic bodies leads to a compensatory increase in neutral lipolysis by Tgl3 and Tgl4 in stationary phase grown yeast which highlights crosstalk between yeast lipophagy and the neutral lipolysis pathways[49].

Table 1. Published pathway components tested for roles in yeast lipophagy. Pathway components tested for roles in yeast lipophagy are classified as positive and negative regulators of lipophagy or as having no effect on the process. Analysis was done using genetic deletion mutants or with chemical inhibitors of cellular components. All listings are for *S. cerevisiae* unless otherwise specified. Temporal conditions for each induction mode may vary between different publications and are not specified here.

Mode of lipophagy induction	Role in lipophagy	Pathway component	Refs
Stationary Phase	**Positive**	*ATG1, ATG2, ATG3, ATG4, ATG5, ATG6, ATG7, ATG8, ATG9, ATG10, ATG12, ATG13, ATG14, ATG15, ATG16, ATG17, ATG18, ATG21, ATG22, ATG23, ATG24, ATG26, ATG27, ATG29, ATG31, ATG32, ATG34, ATG36, FAB1, VPS4, NEM1, PEP4*	22
		NPC2, NCR1	23
		LDO16, LDB16	29
		CUE1, UBC7, RNP1, LHS1, YPT31, VPS34, EGO1, EGO2, CUE4, UBC12, SSA3, SSB2, SSE1, SSE2, TGL4, YPR147C, YPT11, HAL5, KKQ8, NPR1, GAL83, BMH1, RTG1, VPS38, YVC1, MSI1, HAT2, HTA1, NPC2, ATG15	18 (Chapter 4.1)
		PIK1, STT4, VPS27	46
		ATG1, ATG2, ATG3, ATG4, ATG5, ATG6, ATG7, ATG8, ATG9, ATG17, ATG18, ATG26, ATG28, ATG40, YPT7, PEX3, PEX19, VAM7, VPS15, PRL1, Proteinases A,B	26 (*K. phaffii*)
	No effect	*ATG11, ATG19, ATG20, ATG33*	22
		LDO45	29
		YPT6, HSP82, SSA3, CUE5	18 (Chapter 4.1)
		LSB6	46
		ATG11, ATG20, ATG24, ATG25, ATG30, ATG32, ATG35, ATG37, VAC8, APE1, VPS17, UVRAG	26 (*K. phaffii*)
		CUE5	50 (*K. phaffii*)
	Negative	*NVJ1*	51
SD-N	**Positive**	*ATG1, ATG3, ATG4, ATG5, ATG6, ATG7, ATG8, ATG9, ATG10, ATG11, ATG12, ATG14, ATG15, ATG16, ATG17, ATG18, VPS34, YPT7, VAM7, VAM3, TRS85, VAC8, NYV1,* Tubulin	17
		NPC2, NCR1, Actin, *VPS4*	23
		PIK1, STT4	46
		SNF7, VPS27	28
	No effect	*ATG1, ATG2, ATG3, ATG4, ATG5, ATG6, ATG7, ATG8, ATG9, ATG17, ATG18, VPS15, VAM7, YPT7,* Proteinase A,B	26 (*K. phaffii*)
		ATG20, SHP1, VPS38, KRE11, ELO1, ELO3, SLT2	17
		Tubulin	23
		LSB6	46
		ATG11, ATG20, ATG24, ATG25, ATG26, ATG28, ATG30, ATG32, ATG35, ATG37, ATG40, VAC8, APE1, UVRAG, VPS17, PRL1, PEX3, PEX19	26 (*K. phaffii*)
Acute glucose reduction	**Positive**	*SNF1, SNF4, ATG1, ATG2, ATG3, ATG5, ATG6, ATG7, ATG8, ATG9, ATG10, ATG12, ATG13, ATG14, ATG15, ATG16, ATG17, ATG18, ATG23, ATG27, ATG29, ATG31, ATG32, ATG33, ATG34, ATG36*	21
		TGL3, TGL4, YPT7	28
	No effect	*ATG11, ATG19, ATG20, ATG21, ATG22, ATG24, ATG26*	21
	Negative	*VPS27, SNF7, VPS4, VPS21*	28

Lipid/ER stress	**Positive**	*PEP4, ESM1*	25
		VPS4, VPS27, VPS23, VPS36, SNF7, VPS33, VAM3, YPT7	24
		NPC2, NCR1 (PC imbalance induced lipophagy)	27
	No effect	*ATG7*	25
		ATG1, ATG8	24
		NPC2, NCR1 (DTT, TM induced lipophagy)	27
Diauxic shift	**Positive**	*PEP4, VPS27*	52
	No effect	*ATG1*	52

1.6 Objective

When I began this project the knowledge base for the mechanisms and genetic regulators of lipophagy was in its infancy. To address this, I sought to develop a library for the high-throughput identification of the genetic determinants of lipophagy in budding yeast – an organism where several early lipophagy studies, and much of the initial characterization of autophagy was conducted[53]. Furthermore, while there have been studies assessing lipophagy in mammalian cells, the small size of lysosomes can make analysis difficult. The yeast vacuole is much larger and makes analysis of LD interactions with it by microscopy much simpler. Thus, my objective was **to utilise the high-throughput capacity of yeast genetics to develop a library of non-essential single-gene deletion strains in *S. cerevisiae* for the identification of genetic regulators of lipophagy.** A similar library for mitophagy in yeast was previously constructed lending support to my ability to have success with constructing and screening a lipophagy library[54]. As shown in the previous section, our understanding of lipophagy has continued to grow in the subsequent years - to which this work has contributed as will be demonstrated - but there is still a need for the lipophagy library I have developed herein to expedite the scientific understanding of the genetic determinants of lipophagy going forward.

1.7 Paths of investigation for yeast lipophagy regulators

There were two notable groups of genes that my group had interest in exploring lipophagy roles for outside of the screening approach we took. These were the Oxysterol binding protein homolog (OSH) family and genes involved in aggrephagy/aggresome formation. The OSH proteins are involved in regulating sterol and lipid transfer within yeast[55]. Therefore, I have hypothesised that this protein family may regulate lipophagy through the formation of vacuolar microdomains, which are abundant in ergosterol and membrane phospholipids. Lending support to this hypothesis is that lipophagy already relies on other forms of lipid/sterol transport within the cell, as was described with Npc2 and Ncr1 trafficking vacuolar ergosterol[23], Pik1 and Stt2 reorganizing PtdIns(4)P lipids within the vacuolar membrane[46], the involvement of sterol trafficker, Lam6, in vacuolar microdomain formation in other conditions of cell stress[48], as well as vesicular trafficking of membrane and sterol through autophagy and the ESCRT pathway[17,21–23,28]. Therefore, it seems possible that the OSH family may also regulate lipophagy as well. The mammalian oxysterol binding protein (OSBP) can bind oxysterols through its OSBP related domain (ORD) and regulate cholesterol metabolism[56,57]. Additionally, OSBP possesses a pleckstrin homology (PH) domain that allows for PtdIns(4)P binding[56,57]. OSBP, and other related proteins, function by exchanging sterol for PtdIns(4)P at membrane sites allowing for the redistribution of cellular lipid[56]. There are additional OSBP-related proteins (ORPs) with similarities to OSBP. Notably, ORDs of different ORPs have varying lipid affinities allowing for regulation of cellular lipid metabolism and distribution[56]. As mentioned, the yeast equivalents of the mammalian ORPs are the OSH family of which there are 7 members: Osh1-Osh7. The Osh proteins are cytosolic and mediate lipid transfer between different membranes[56]. Osh1-Osh3 contain PH domains in addition to an ORD and have the most structural similarities to mammalian OSBP[56]. The PH domains interact with

membrane phosphoinositides and target these Osh proteins to different membranes where they can facilitate lipid exchange[56]. On the other hand, Osh4-Osh7 only possess an ORD[56]. Structural analysis of the ORDs in Osh3, Osh4 and Osh6 show a conserved β-barrel structure with a central hydrophobic tunnel where a single lipid molecule is carried during lipid exchange[56,58]. The lipid affinities of the different OSH family members are an active area of investigation. Like OSBP, Osh4 can exchange sterol for PtdIns(4)P within organelle membranes – thus driving sterol transport, which opens the possibility that it may work downstream of the aforementioned phosphatidylinositol 4-kinases, Pik1 and Stt2, in regulating vacuolar membrane lipid content[46,56,59–61]. All members of the OSH family have affinity for PtdIns(4)P through their ORD domains, and it is thought they are all involved in some form of lipid exchange, though a comprehensive look into the lipid affinities for each Osh protein has not been performed[56]. Given the size of the hydrophobic space in the structure of Osh3, it is not believed to have sterol binding affinity and its lipid binding affinities outside of PtdIns(4)P are unknown[56]. It has been reported that Osh4-Osh7 can bind sterol *in vitro*[55]. However, other work suggests that Osh6 and Osh7 can also bind phosphatidylserine (PS) and exchange this lipid with membrane PtdIns(4)P, raising the question of whether sterol transport is a key function of Osh6 and Osh7[57,62]? In support of this, another study shows that Osh2, Osh4 and Osh5 have the highest sterol trafficking levels[56]. As of yet the Osh proteins have not been shown to facilitate lipid exchange at the vacuolar membrane, though we are still interested in investigating the possible roles of this family in lipophagy – possibly through vacuolar microdomain formation. Overall, all OSH family members can bind PtdIns(4)P and many have confirmed sterol binding properties[56]. While the lipid affinities of all the Osh proteins are not yet known they are all putative candidates for lipophagy given their lipid trafficking properties. Therefore, I aimed to test Osh1-Osh7 for roles in lipophagy. We also had

interest in assessing the genes involved in aggrephagy/aggresome formation for roles in yeast lipophagy. As will be explained in detail in Chapter 3.3, our lab performed mass spectrometry on LDs isolated from human macrophage foam cells to identify putative proteins that may regulate lipophagy. Several of these were mediators of aggrephagy, the autophagic form targeting aggresomes, which are aggregations of ubiquitinated protein. Some of these proteins included OPTN, a selective autophagy receptor, HSPA5, a molecular chaperone, TERA, an ATPase, and 14-3-3, a molecular chaperone that recruits misfolded proteins[18]. Furthermore, a recent study showed that dHDAC6, a histone deacetylase and mediator of aggresome formation, regulated the turnover of LDs through p62, an autophagy receptor[63]. Based on these observations we were interested in assessing the yeast genes involved in aggrephagy and aggresome formation for possible roles in lipophagy. The yeast genes tested for this aggrephagy/aggresome component of the screen, and their human homologs/equivalent genes are shown in Table 2.

Table 2. Yeast genes related to aggrephagy/aggresome formation

Gene Name	Function
HDA1	Histone deacetylase and dHDAC6 homolog[64]
CUE5	Ubiquitin binding protein, aggrephagy selective autophagy receptor and TOLLIP homolog[40]
BMH1/BMH2	14-3-3 proteins, a molecular chaperone that recruits misfolded proteins and homologs of mammalian 14-3-3s[65,66]
GVP36	Involved in vacuole biogenesis, actin remodeling, is localized to LDs and is aggregated/degraded by Cue5 selective autophagy[40,67,68]
HSP42	Aggregase for cytosolic protein aggregation[69]
BTN2	Aggregase for nuclear protein aggregation[70,71]
HSP104	Disaggregase that was found to localize with LDs in lipid stress that induced microlipophagy[25]

2.0 Materials and methods

2.1 Non-synthetic genetic array strain construction, growth conditions and media

The query strains used in the lipophagy library construction and select other strains were generated through the PCR-mediated deletion and tagging of genomic DNA, as previously described in Longtine *et al.* 1998[72]. These strains were confirmed via growth on drug selection agar plates containing either: G418 (Wisent Bioproducts, 400–130-IG), nourseothricin (Nat) (MJS Biolynx Inc., JBAB102XL), hygromycin (Hyg) (Wisent Bioproducts, 450–141-XL) or on agar plates lacking histidine, depending on selectable markers listed in the strain genotype information in Table S1, and by PCR. The *Saccharomyces cerevisiae* Deletion Mutant Array (GE, CAT#YSC1053) and GFP collection (Thermo, CAT#95702) were taken from for certain strains as listed in Table S1. For SD-N experiments yeast were grown in YPD media composed of 10g/L yeast extract (Multicell), 20g/L bacteriological peptone (Multicell) and 2% dextrose until OD600 of 0.4 was reached at which point cells were centrifuged, washed and media was changed to synthetic complete (SC)-OA composed of 6.7g/L yeast nitrogen base + ammonium sulfate (multicell), 2.06g/L standard complete amino acid mix, 2% dextrose and 0.1% oleic acid (Fluka) for 15 hours. Cells were centrifuged, washed in autoclaved, distilled water 3 times before being resuspended in SD-N media, composed of 6.7g/L yeast nitrogen base without ammonium sulfate or amino acids and 2% dextrose, for 6h. For stationary phase growth experiments strains were inoculated at an initial OD600 of 0.1 in SC media composed of 6.7g/L yeast nitrogen base + ammonium sulfate (multicell), 2.06g/L standard complete amino acid mix (SC Biomedicals) and 2% dextrose for 5 days. All strains were grown at 30C and at 200RPM in shaking incubator or on rotating wheel.

2.2 Synthetic genetic array mating for library development

Construction of the lipophagy library was done using synthetic genetic array (SGA) mating protocols as previously described[73–75]. Mating was done using a query strain with background Y7092 (Table S1) against the yeast non-essential Deletion mutant array (DMA) library (GE, CAT#YSC1053). Query strain mutations were confirmed by PCR. For high-throughput strain construction of the lipophagy library, the MATα query strain was mated to the MATa deletion mutant array via pinning onto YPD plates with a Singer RoToR HDA (Singer Instruments). Following diploid growth at 30C, plates were repinned onto sporulation media, as previously described[73], and incubated at 25C for 5 days. As described, MATa progeny selection was performed by pinning of sporulated yeast onto SD-His + Canavanine plates followed by growth at 30C[73]. This was followed by successive rounds of pinning onto chemical selection YPD plates with Nat (Faa4-GFP), Hyg (Vph1-mRuby2) or G418 (DMA genetic deletions) to select for final haploid strains with each mutation, as previously described[73–75].

2.3 Confocal microscopy

Confocal microscopy imaging was performed on a ZEISS LSM 880 using the Airyscan module with the 63x oil objective. For stationary phase experiments, imaging was performed at the day 1 (D1) timepoint – 24h following initial inoculation and at day 5 (D5) - 120h following inoculation. For the SD-N experiments imaging was performed following the 6h of SD-N treatment. For these experiments yeast growths were centrifuged at the specified timepoints and most supernatant media was removed. Yeast was then resuspended in the remaining media and added to a microscopy slide for imaging. For strains lacking a genomic vacuolar fluorescent tag, the vacuolar

dye - FM 4-64 (Molecular probes) was added at a final concentration of 40uM at the stage of initial inoculation or an alternate vacuolar dye - Celltracker Blue CMAC dye (Thermo C2110) was added at a final concentration of 20uM prior to imaging for 20 minutes. For staining of LDs in strains lacking a genomic *FAA4* or *ERG6* fluorescent protein tag, either 50uM of monodansylpentane (MDH) (Abcepta SM1000a) or 0.5ug/mL of BODIPY FL neutral lipid dye (Invitrogen D3922) were added for 10 minutes prior to centrifugation of the samples before imaging, as previously described[22,25]. During imaging, single plane images were captured at the plane at which the vacuolar diameter was its widest. Quantification of LDs inside/outside vacuoles was manually performed on images. The quantification of this imaging was done with different grades of LD-vacuolar internalization. As previously used by Wang *et al.* (2014) these levels would be LDs inside the vacuole = 0, LDs inside the vacuole = 1 - 2, and LDs inside the vacuole ≥ 3[22].

2.4 Imunoblotting

Faa4-GFP vacuolar cleavage assays were performed on stationary phase grown yeast strains. Samples were collected at the same times as the D1 and D5 timepoints for confocal microscopy. Following centrifugation, supernatant was removed, and pelleted yeast cells were flash frozen in liquid nitrogen for 5 minutes before storage at -80C prior to sample processing. Yeast pellets were then washed with PBS and lysed directly in 2x Laemmli sample buffer (BioRad, 1610737) and boiled at 95C for 15 min. Samples were electrophoresed on 12% TGX Stain-Free™ FastCast™ Acrylamide gels (BioRad, 1610185). Gels were activated and transferred to 0.22 μm PVDF membranes for 10 min using the Trans-Blot Turbo Transfer System (BioRad). Stain-free blots were visualized and imaged to be used for protein normalization. Membranes were then blocked

in 5% milk in TBST for 1 h. Membranes were probed with anti-GFP (1:1000; Novus Biologicals, NB600-308). Proteins were detected using an enhanced HRP-based chemiluminescence detection system (HRP-conjugated secondary antibodies from Amersham Biosciences [NA931V]) and Clarity or Clarity Max Chemiluminescence Reagent from BioRad (1705060, 1705062) using a ChemiDoc XRS+ System (BioRad). Membranes were washed in TBST pre and post addition of secondary antibody. Densitometry of bands was analysed using Imagelab (BioRad) to compare free GFP levels.

2.5 Colocalization analysis

Fluorescent channels corresponding to the Osh-GFP and FM 4-64 labels of the confocal microscopy images were thresholded using ImageJ software and a mask was applied. The JACOP plugin was then used to assess the degree of colocalization between the two channels and data was graphed using the thresholded Manders colocalization coefficients.

2.5 Statistical analysis

Lipophagy comparisons for experiments where at least n=3 is shown were done using two-way ANOVA with either Tukey, Dunnett or Sidak multiple comparison testing. Comparisons of LD level at D1 for the *OshΔ* mutants was done using one-way ANOVA with Dunnett multiple comparison testing.

3.0 Results

3.1 Stationary phase growth induces lipophagy to a high level compared to nitrogen starvation

I first developed a *S. cerevisiae* strain that could be used for the quantification of lipophagy. Starting from the synthetic genetic array (SGA) query strain Y7092 (Table S1) that would be used for mating against the yeast deletion mutant array (DMA) – a library that contains single gene deletions of the entire *S. cerevisiae* non-essential genome – PCR site directed mutagenesis, described in Longtine *et al.* (1998) was used to incorporate the genetic sequence encoding an eGFP fluorescent protein onto the C-terminal chromosomal locus of *FAA4*, which encodes a fatty acyl-CoA synthetase, and is well established as an LD coat protein[17,72]. In addition to this, I used this same method to incorporate the gene of an mRuby2 fluorescent protein onto the C-terminal chromosomal sequence of *VPH1*, which encodes a vacuolar ATPase component, and is established as a marker of the vacuolar membrane[21,22]. With these two markers I was able to monitor interactions between LDs and the vacuole allowing for assessments of lipophagy via confocal microscopy. At the time I began this project there were two main methodologies of inducing lipophagy in *S. cerevisiae*: SD-N and stationary phase growth, as described in Van Zutphen *et al*. (2014) and Wang *et al.* (2014), respectively[17,22]. I sought to determine which of these methodologies showed the strongest activation of lipophagy that could be attenuated in genetic deletion yeast strains for known *ATG* genes previously reported to be indispensable for lipophagy (Table 1). Specifically I used an *atg8Δ* deletion strain that was previously shown to be impaired for lipophagy in both SD-N and stationary phase growth conditions[17,22]. This autophagy deletion strain was generated using PCR site directed mutagenesis, as well, to incorporate an antibiotic resistance cassette, *KanMX4*, which allows for resistance to the G418 drug, into the chromosomal

reading frame of the desired gene. Despite findings from previous publications, our observations by confocal microscopy in strains containing the *FAA4-GFP VPH1-mRuby2* genetic markers following oleic acid lipid loading to induce LD biogenesis followed by 6h of SD-N (SD-N) showed no significant levels of LD internalization into the vacuole for either the wild-type or the *atg8Δ* strain (Figure 2A). By contrast, growth to D5 of the stationary phase in synthetic complete (SC) nutrient rich media led to a significant increase in lipophagy in the wild-type strain that was attenuated in the *atg8Δ* strain (Figure 2B). Because I observed this strong induction of lipophagy in the stationary phase that matched findings from previous work, I elected to move forward with our genetic screen of yeast lipophagy with stationary phase growth as the induction method[22].

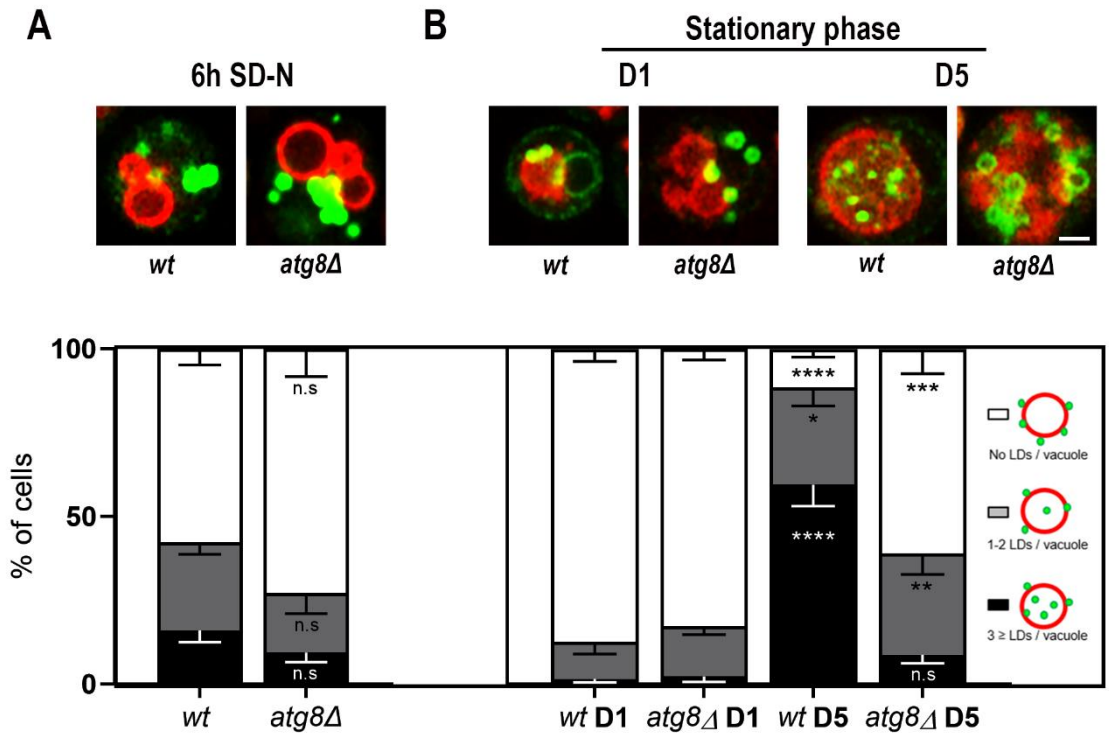

Figure 2. Stationary phase growth but not SD-N activates lipophagy. A) *FAA4-GFP VPH1-mRuby2* wild-type and *atg8Δ* yeast were imaged for lipophagy following oleic acid lipid-loading and 6h SD-N (n=3). B) *FAA4-GFP VPH1-mRuby2* wild-type or *atg8*Δ yeast were imaged by confocal microscopy for lipophagy (n=7) after D1 or D5 growth in SC media. Green fluorescent signal corresponds to LDs (Faa4-GFP) and red fluorescent signal corresponds to the vacuole (Vph1-mRuby2). Scale bar represents 2uM. For A) statistical testing was done by two-way

ANOVA with Sidak multiple comparisons test. For B) statistical testing was done by two-way ANOVA with Tukey multiple comparisons test with significance for each strain being shown in comparison to wild-type D1. Statistical significance level is **** ($p \leq 0.0001$).

3.2 The Rosella autophagy biosensor was unable to detect lipophagy

In addition to using the *FAA4-GFP* and *VPH1-mRuby2* markers to assess lipophagy I also sought to develop a strain that could be used for high-throughput quantification. I was intrigued by an autophagy biosensor, known as Rosella, that was previously described in *S. cerevisiae* and had been used to assess mitophagy, piecemeal microautophagy of the nucleus and general bulk autophagy[76–78]. This biosensor showed promise for its ability to detect autophagy via flow cytometry and could enable a high-throughput analysis of lipophagy for our work[76]. Rosella is comprised of two fluorescent proteins in tandem: DsRed.T3, a pH stable RFP variant and SEpHluorin, a pH sensitive GFP mutant[76]. SEpHluorin is unable to emit fluorescence in environments of pH ≤ 6.0[79]. The biological relevance of this to autophagy is that the pH of the yeast vacuole is approximately 6.0[80]. Following internalization of Rosella by the acidic yeast vacuole, the fluorescence emission of SEpHluorin is quenched, while that of DsRed.T3 is unchanged (Figure 3A)[76]. To assess lipophagy using Rosella, it was tagged onto the C-terminal end of the chromosomal locus of *ERG6*, which encodes a delta (24)-sterol C-methyltransferase and well-established LD coat protein[17]. It is worth noting that we attempted tagging of *Rosella* onto *FAA4* to match our validated lipophagy strain containing the *FAA4-GFP* marker, however, this was not successful. Comparisons in the literature as well as our own work show that the fluorescence of LDs tagged from Faa4 or Erg6 is identical[17,22]. Assessment of the *ERG6-Rosella* strain under late stationary phase growth (D5) failed to show activation of lipophagy in wild-type yeast, evidenced by the absence of either Erg6 fluorescent signal within vacuoles, as labeled with 7-amino-4-chloromethylcoumarin (CMAC), or regions of sole Erg6-DsRed.T3 expression which

would indicate SEpHluorin quenching and active lipophagy (Figure 3B). These same observations were made for the *atg8Δ* strain. It is possible that the large size of the Rosella tandem fluorescent protein impaired LD ability to undergo lipophagy. Regardless, I concluded that lipophagy could not be accurately assessed using Rosella in our model and thus did not pursue it further.

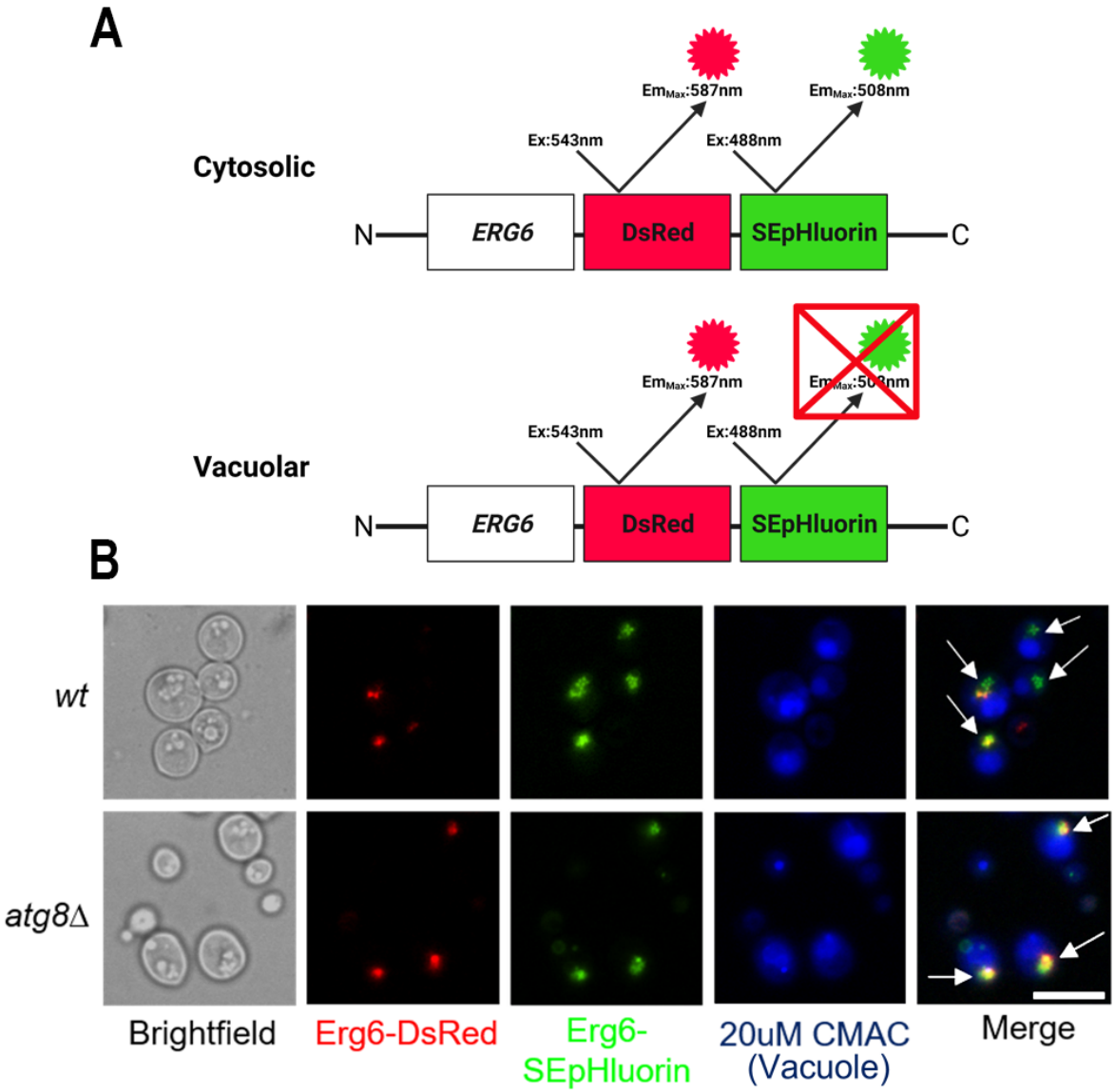

Figure 3. Erg6-Rosella is not able to detect stationary phase lipophagy in *S. cerevisiae*. A) Schematic representing expected Erg6-Rosella fluorescent properties in different cellular compartments. B) Wild-type and *atg8*Δ yeast strains expressing Erg6-Rosella were grown in SC media into the late stationary phase (D5). Vacuoles were labelled with 20uM CMAC prior to imaging. White arrows indicate Erg6 signal (LDs) outside of vacuoles. Scale bar represents 10uM.

3.3 A single-gene deletion library for the assessment of lipophagy in *S. cerevisiae* was developed

Having established the *FAA4-GFP VPH1-mRuby2* genetic markers to assess lipophagy I sought to develop a library of single-gene deletion strains of the non-essential genome of *S. cerevisiae* containing these markers that I could then screen for lipophagy roles. This would be done by mating my query strain developed in Chapter 3.1 against the DMA. To do this I used SGA technology. SGA technology allows for high-throughput construction of libraries of yeast containing multiple mutations through the genetic crossing of a query strain with an existing yeast library. To better understand the details behind the SGA methodology the basics of the yeast life cycle will be explained. Yeast can exist as one of two haploid cell types:**a** and α, which refer to the yeast mating type as governed by genetic differences at the *MAT* chromosomal locus (*MAT***a***/MATα)*[81]. Haploid yeast, which are the ploidy of all yeast used in this work for experimentation, proliferate through mitotic division but can also mate with yeast of the opposite mating type which leads to nuclear fusion and the formation of one diploid zygote cell (Figure 4)[73,75,81]. Yeast mating operates through chemotaxis. Each mating type secretes a pheromone, either a-factor or α-factor pheromone, which binds onto a G-protein coupled receptor (GPCR) of the opposite mating type, either Ste2 for *MAT***a** or Ste3 for *MATα*[81]. Pheromone binding triggers a MAP-kinase signal transduction cascade that leads to mitotic arrest, formation of a mating projection towards the source of the other haploid, and cell/nuclear fusion[81]. Sporulation of the diploid zygote yeast, induced by nutrient limitation, generates four new haploid yeast spores through meiosis that due to the law of segregation will have a random combination of alleles from the initial *MAT***a** and *MAT*α strains[82]. Growth on a nutrient rich media again allows for the germination of these haploid spores back into haploid yeast[81]. In practice, I used a robotic pinning

machine to mate the haploid *MATα* query strain I developed containing the *FAA4-GFP VPH1-mRuby2* genetic markers and the haploid *MAT***a** DMA together, which generated a diploid library containing *FAA4-GFP*, *VPH1-mRuby2* and a deleted DMA gene (*geneXΔ*), plus wild-type copies of each of these genes (Figure 4). Spores were generated by pinning the library onto carbon/nitrogen poor plates and grown at 25C (Figure 4)[73] after which I selected for *MAT***a** yeast using the *can1Δ::STE2pr-SP-his5* genomic modification that is present in the Y0792 query strain background[73]. This strain, which cannot synthesise histidine on its own, has a genetic cassette (*SP-his5)* added allowing for histidine production. This cassette has also been added to replace the *CAN1* gene[73] and is under control of the *STE2* promoter and therefore will only be active in *MAT***a** yeast. Thus, only *MAT***a** haploids will produce histidine and survive on selection plates lacking histidine. The drug canavanine is also used as a selection drug as it is lethal to yeast in which the *CAN1* gene is intact. Therefore any remaining diploid yeast expressing *CAN1* will be removed from the population[73]. I then used Subsequent rounds of chemical selection to isolate the *MAT***a** haploid yeast that contained all the desired *FAA4-GFP, VPH1-mRuby2* and *geneXΔ* genotypes (Figure 4). Specifically, the *FAA4-GFP* marker was linked with a *NatMX6* cassette (*FAA4-GFP::NatMX6)* conferring resistance to the nourseothricin (Nat) antibiotic, the *VPH1-mRuby2* marker with an *hphMX6* cassette (*VPH1-mRuby2::hphMX6)* conferring resistance to the hygromycin (Hyg) antibiotic and the DMA has deleted the yeast non-essential genome using the *KanMX4* cassette conferring resistance to the G418 drug[73]. These genotypes are shown in Table S1. These rounds of chemical selection yielded my final lipophagy library that is ready for screening (Figure 4).

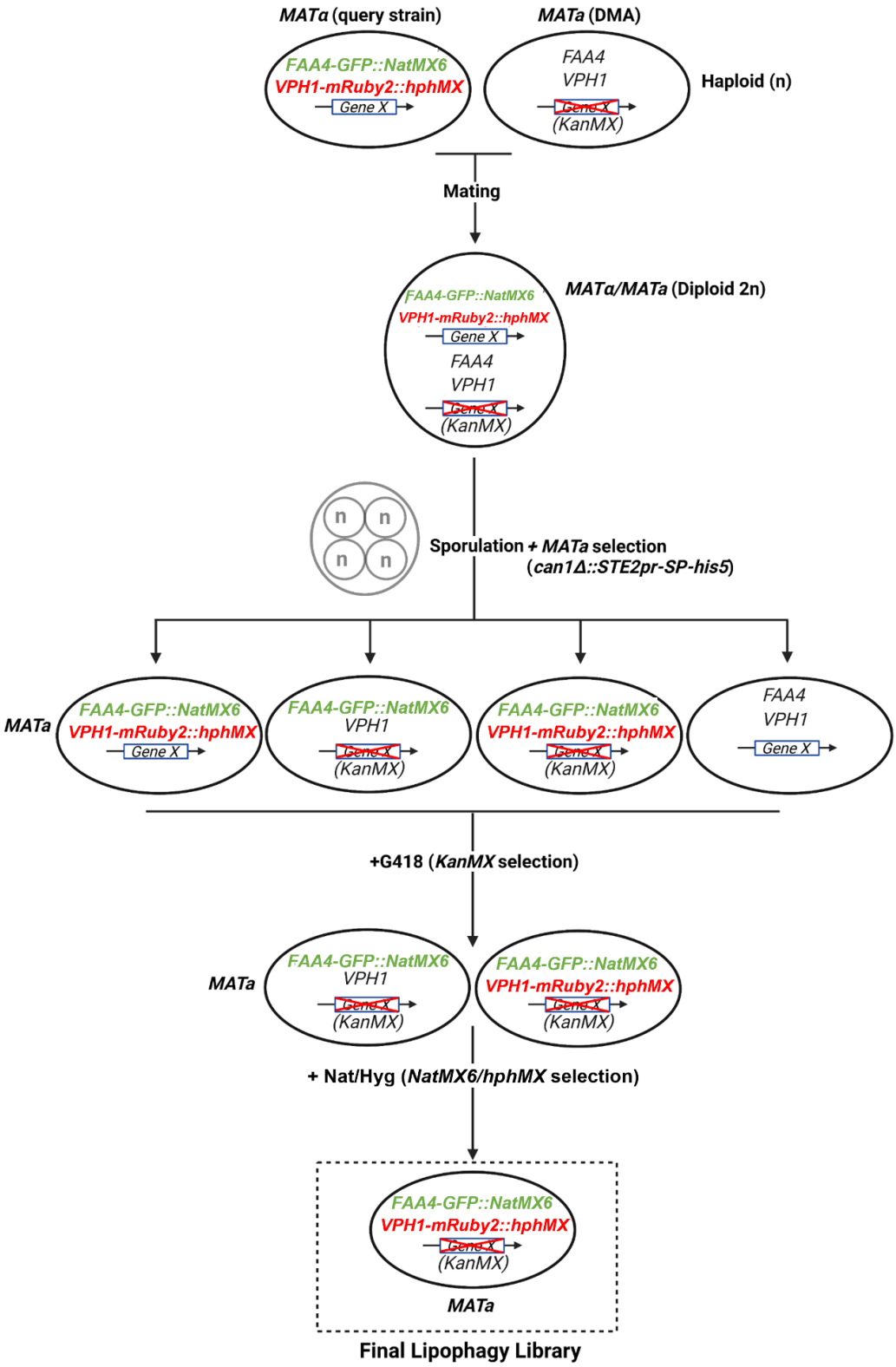

Figure 4. SGA mating methodology used to develop the lipophagy library. Schematic is shown for one representative gene of the DMA (*GeneX*). Nat stands for nourseothricin and Hyg stands

for hygromycin.

3.4 Screening of yeast homologs/genes of similar function to macrophage putative lipophagy regulators identified multiple novel regulators of lipophagy in *S. cerevisiae*

I began the investigation into the lipophagy regulators of *S. cerevisiae* by looking at the yeast homologs or genes of related function of putative lipophagy proteins that were identified on the surface of LDs isolated from macrophage foam cells. Briefly, other members of the lab lipid loaded THP-1 human macrophages with aggregated LDL to stimulate LD biogenesis and treated them with the general autophagy inhibitor, chloroquine, or not[18]. LDs were isolated through ultracentrifugation and mass spectrometry was performed to analyze the proteomes of the two populations of LDs. There were several protein candidates enriched in the chloroquine treatment – when lipophagy is impaired – suggesting putative roles in this process[18]. Furthermore, other proteome candidates with known roles in biological processes that may be related to lipophagy, and autophagy were considered putative lipophagy regulators as well. With this initial list of macrophage putative lipophagy candidates I began identifying the yeast homologs or genes of similar function so that I could assess the roles of these genes in *S. cerevisiae* lipophagy. To do this I used a combination of the *Human gene to yeast homolog* option on the YeastMine program found within the *Saccharomyces* Genome Database (SGD) as well as OrthoMCL 2.0b6, an ortholog identification program. In cases where no yeast equivalent genes were identified by these softwares, and to supplement the results of these softwares, literature analysis was performed to identify homologs or close gene equivalents based on structure, function, and protein motifs. Table 3 highlights many of the putative macrophage lipophagy genes that our lab identified as well as the corresponding yeast equivalent genes for which there were deletion strains in my final lipophagy library. I then performed confocal microscopy to assess the internalization of Faa4-GFP

labeled LDs into the Vph1-mRuby2 labeled vacuoles, as previously described, on a select number of deletion yeast strains grown into D5 of the stationary phase to induce lipophagy (Figure 5B). Quantification of this microscopy (Figure 5A), shown as a representative experiment of n=3 performed, as well as representative images of these strains (Figure 5B) highlights genes that are both possible positive regulators of lipophagy – as represented by lower levels of vacuolar internalization in comparison to the wild-type in the genetic deletion strain, and as possible negative regulators of lipophagy – as represented by higher levels of vacuolar internalization in comparison to the wild-type in the genetic deletion strain. There are also deletion strains that show comparable lipophagy levels to the wild-type indicating these genes are dispensable for the process of stationary phase induced lipophagy. Throughout our lipophagy screening in *S. cerevisiae* the *atg8Δ* strain, and known positive regulator of lipophagy, is carried alongside the wild-type strain as a control to ensure the lipophagy levels are comparable between experiments. There were several important lipophagy gene observations from this confocal microscopy analysis. Notable *S. cerevisiae* genes showing lower levels of LD internalization into the vacuole in the deletion strain in comparison to the wild-type (Figure 5AB) include (Human equivalents listed in parentheses): *LHS1* (HSPA5), *RNP1* (CIRBP), *UBC7* (UBE2G2), *CUE1* (AUP1), *NPC2* (NPC2) and *YPT31* (RAB2A). Notable genes showing higher level of LD internalization into the vacuole in the deletion strain include: *YPT6* (RAB6), *SSA3* (HSPA8), and *ATG15* (LAL) (Figure 5AB). The deletion strains for *CUE5* (TOLLIP) and *HSP82* (HSP90AA1) did not show differences in LD internalization into the vacuole in comparison to the wild-type (Figure 5AB). These findings will be explained further in Chapter 4.1. In addition to confocal microscopy to assess lipophagy we performed Faa4-GFP vacuolar cleavage assays via immunoblotting. These are well established yeast assays to assess vacuolar degradation of various cargos, and by extension, different selective

autophagies[17,21–27,83,84]. The principle is that cellular proteins tagged with GFP, when targeted to the vacuole, will undergo hydrolysis. However, GFP is more resistant to vacuolar degradation and the ratio of the free GFP to the fusion protein can be used as a metric of autophagic flux. Therefore, the level of free GFP resulting from vacuolar cleavage of the Faa4-GFP fusion protein can be used to assess lipophagy during the stationary phase. Validation of this methodology is shown in Figure 5C where the presence of a free GFP band indicates active lipophagy in the wild-type strain that is lost in the *atg8Δ, atg9Δ* and *atg32Δ* deletion strains which corroborates previous work[22]. However, I did not observe this lipophagy impairment in the *atg21Δ* strain in contrast to previous findings[22]. Following validation of this methodology we tested additional yeast homologs/genes of similar function to putative macrophage lipophagy candidates with a Faa4-GFP cleavage assay-based screen. Observations from this screen are shown in Table 3, where GFP cleavage is shown as the trend of ≥3 out of 4 independent experiments. These results will be further elaborated upon Chapter 4.1, but it is apparent that screening of the lipophagy library has identified a wide variety of genes whose deletion strains show lower levels of free GFP in comparison to the wild-type and appear to positively regulate stationary phase induced lipophagy in yeast (Table 3).

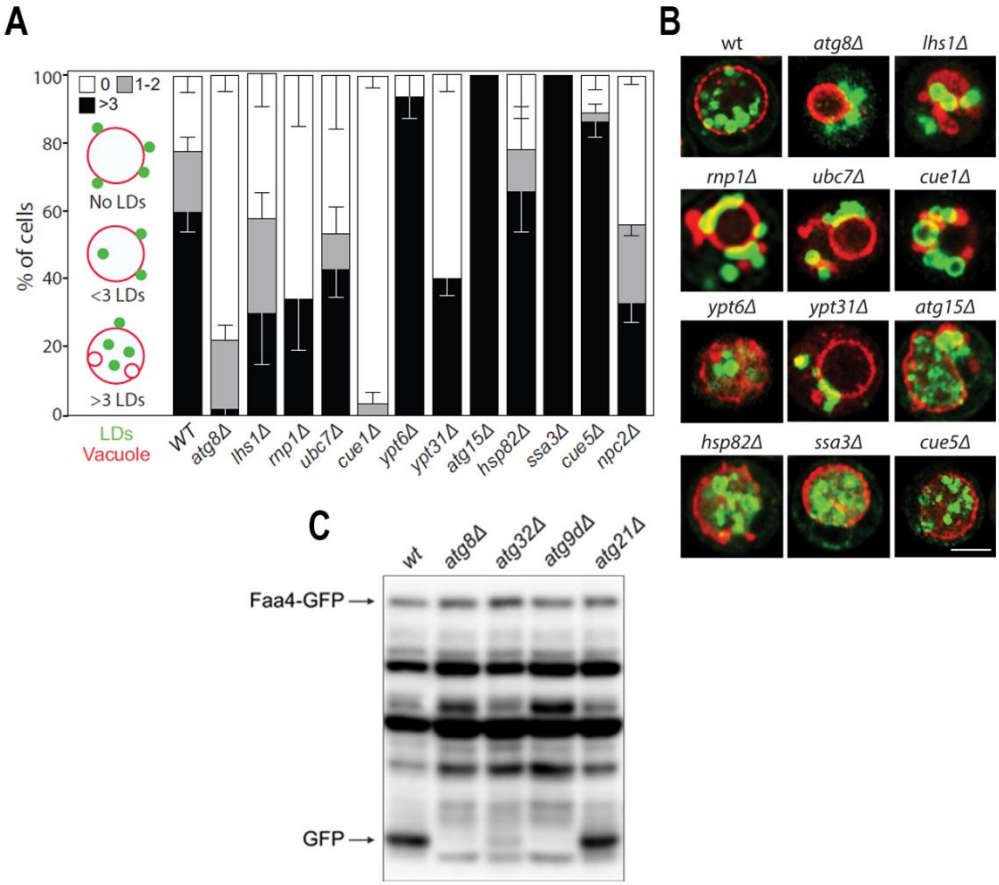

Figure 5. Identification of novel lipophagy regulators from the yeast equivalents of putative lipophagy candidates from macrophages. A) Quantification of late stationary phase lipophagy (D5) for single-gene deletion yeast from the lipophagy library. Quantification of a representative experiment is shown of n=3 performed. B) Representative confocal microscopy images of strains corresponding to those in A). Green fluorescent signal corresponds to LDs (Faa4-GFP) and red fluorescent signal corresponds to vacuoles (Vph1-mRuby2). Scale bar represents 5uM. C) Faa4-GFP cleavage for strains grown to the late stationary phase (D5). Bands for the Faa4-GFP fusion protein and free GFP are highlighted.

Table 3. Faa4-GFP vacuolar cleavage screen of yeast deletion strains. Original human putative lipophagy genes are listed in comparison. Faa4-GFP vacuolar cleavage is shown as the free GFP level relative to the wild-type strain as the trend of 3 out of 4 independent experiments. Blots correspond to samples grown to D5 of the stationary phase.

Yeast Mutant	Human homolog/gene of similar function	Molecular Function	Free GFP level
atg8Δ	MAP1LC3A	Autophagosome formation	Low
vps34Δ	PIK3C3	Autophagosome formation	Low
ego1Δ	LAMTOR5	Metabolic regulator of autophagy	Low
ego2Δ	LAMTOR5	Metabolic regulator of autophagy	Low
cue4Δ	AUP1	Ubiquitin conjugation	Low
ubc12Δ	UBE2G2	Ubiquitin conjugation	Low
ssa3Δ	HSPA8	Molecular chaperone	Low
ssb2Δ	HSPA5	Molecular chaperone	Low
sse1Δ	HSPH1	Molecular chaperone	Low
sse2Δ	HSPH1	Molecular chaperone	Low
tgl4Δ	PNPLA2	Triglyceride hydrolysis	Low
ypr147cΔ	LDAH	Lipid hydrolysis	Low
ypt31Δ	RAB2	Vesicular trafficking	Low
ypt11Δ	RAB10,13	Vesicular trafficking	Low
hal5Δ	PRKAA1	Cellular energy homeostasis	Low
kkq8Δ	PRKAA1	Cellular energy homeostasis	Low
npr1Δ	PRKAA1	Cellular energy homeostasis	Low
gal83Δ	PRKAA1	Cellular energy homeostasis	Low
bmh1Δ	YWHA	Signaling protein	Low
rtg1Δ	TFEB	Autophagy transcription factor	Low
vps38Δ	UVRAG	Autophagy initiation	Low
yvc1Δ	MCOLN1	Late endocytic trafficking	Low
por2Δ	VDAC2	Autophagy suppressor	High
msl1Δ	RBBP7	Cell proliferation	Low
hat2Δ	RBBP7	Cell proliferation	Low
hta1Δ	MACROH2A1	Nucleosome structure	Low

3.5 Additional screening in *S. cerevisiae* identified further lipophagy regulators

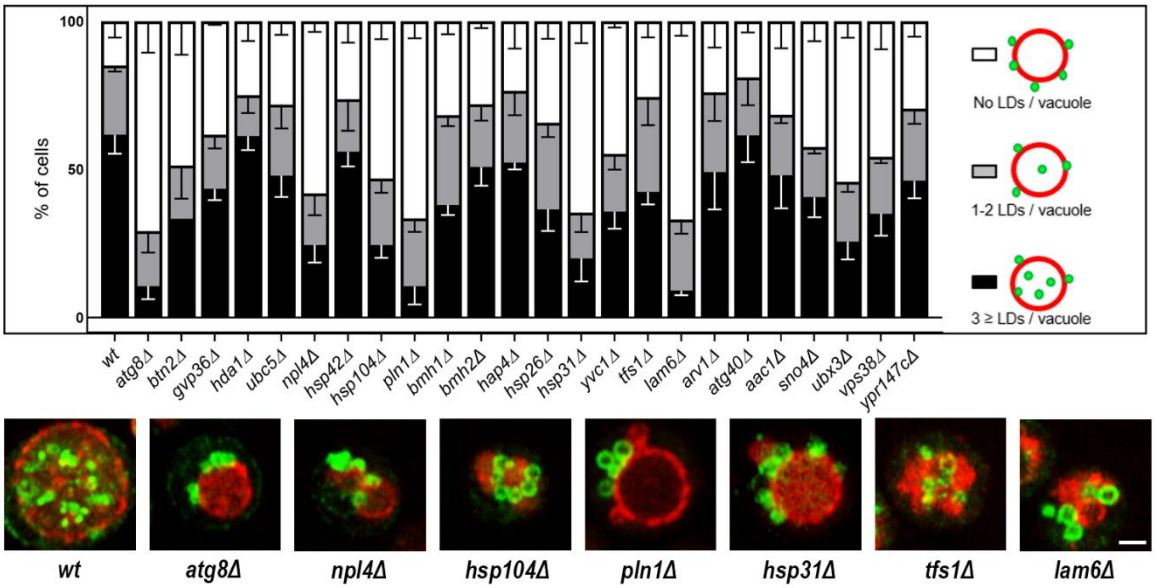

Figure 6. Further screening in *S. cerevisiae* identified deletion strains where stationary phase lipophagy is impaired. Deletion strains taken from the lipophagy library were assessed for roles in stationary phase lipophagy. Quantification of lipophagy levels at the late stationary phase (D5) is shown (n=1 for each strain). The *bmh1Δ* and *bmh2Δ* strains are n=2. Representative confocal microscopy images are shown for strains with notable lipophagy defects. Green fluorescent signal corresponds to LDs (Faa4-GFP), and the red fluorescent signal corresponds to the vacuole (Vph1-mRuby2). Scale bar represents 2uM. Data is presented as mean of each strain with error bars showing the SEM of the image sampling.

Following the initial assessment of the yeast homologs of the putative lipophagy regulators identified in macrophage foam cells, I sought to identify additional novel lipophagy regulators by screening genes based on previously identified roles in the literature. I started this by performing gene ontology (GO) term analysis on the entire *S. cerevisiae* non-essential genome. This was done using the *Gene ontology term finder* software found within the SGD. Each gene was classified by its molecular function or a component of the cell it is associated with. Genes assigned to lipophagy relevant GO terms, such as: autophagy, vacuole, sterol transport and lipid binding were chosen for screening. Additionally, I performed literature analysis to supplement this classification by identifying yeast genes associated with aggrephagy/aggresome formation as mentioned in chapter

1.7, as well as lipid droplet associated genes that we hypothesise may also be involved in lipophagy regulation. In addition to the previously described aggrephagy components, other notable proteins that I aimed to assess for roles in lipophagy include: Pln1, the sole yeast perilipin involved in LD biogenesis and stability[85], Bmh2, another yeast 14-3-3 homolog[66], Hsp26, another molecular chaperone[69], Hsp31, involved in stationary phase survival and shares similarities to mammalian PARK7 (a putative macrophage lipophagy regulator found on the LD proteome in our previous work)[86], Tfs1, a protein involved in stationary phase survival[87], Lam6, the aforementioned sterol transporter[48], Atg40, an autophagy receptor involved in ERphagy and one of the only Atg protein not previously tested for roles in lipophagy to date[88,89], and Ubx3, an endocytosis regulator[90]. I then tested these components for roles in stationary phase lipophagy via confocal microscopy using the deletion strains of the lipophagy library (Figure 6). Because this was initial screening work for many of these genes, only n=1 has been completed for most of the strains shown, except for *Bmh1Δ* and *Bmh2Δ* which are n=2. This secondary screen provides an initial understanding of how these genes may regulate yeast stationary phase induced lipophagy. Observations from this microscopy show that in comparison to the wild-type strain the *btn2Δ, npl4Δ, hsp104Δ, pln1Δ, hsp26Δ, hsp31Δ, yvc1Δ, lam6Δ*, *ubx3Δ,* and *vps38Δ* deletion strains show marked impairments in LD internalization into the vacuole following growth to D5 of the stationary phase (Figure 6). The deletion strains of *gvp36Δ, bmh1Δ, tfs1Δ, sno4Δ* and *ypr147cΔ* show more moderate impairments in LD internalization into the vacuole following growth to D5 of the stationary phase. There are other deletion strains that show no differences in lipophagy compared to the wild-type strain. Notable deletion strains of this phenotype are *hda1Δ, bmh2Δ, hsp42Δ* and *atg40Δ* (Figure 6). These findings will be elaborated upon further in Chapter 4.2.

3.6 Members of the OSH family in yeast show vacuolar localization and involvement in lipophagy

As mentioned previously, our group was independently interested in studying the role of ORPs within lipophagy given their lipid and sterol trafficking abilities, thus I also sought to test the OSH family yeast homologs for roles in *S. cerevisiae* lipophagy. This rationale was further supplemented as many of the OSH members appeared in the GO term analysis of the DMA – corresponding with lipophagy relevant terms like: lipid transport, sterol transport, autophagy, and vacuolar transport. I performed confocal microscopy analysis on the single-gene *OshΔ* deletion strains from my lipophagy library as previously described. However, the *Osh4Δ* was not generated in my initial SGA mating procedures, therefore this strain was obtained from the unmated DMA collection and labeled with the lipophilic BODIPY FL dye for LDs and FM 4-64 for the vacuole (Figure 6B). I first assessed whether the *Osh* mutants impaired LD biogenesis at D1 of the stationary phase, a condition in the wild-type yeast that induces LD proliferation[31]. This was to assess whether Osh components are affecting LD biology outside of lipophagy given their widespread roles in the trafficking of sterol and other lipids - components of the LD neutral lipid core. I did not observe any significant impairments in LD number at D1 of the stationary phase (prior to lipophagy activation) in any of the *OshΔ* strains, suggesting these mutants do not affect LD biogenesis (Figure 7A). Confocal microscopy analysis of these single-gene mutants at D5 of the stationary phase (n=3) when lipophagy is active show that compared to the wild-type strain, only the *Osh7Δ* shows statistically significant impairments in LD internalization into the vacuole (Figure 7BC). The *Osh3Δ* and *Osh4Δ* deletion strains are trending towards statistical significance for impairments in lipophagy in these conditions. I did not observe differences in lipophagy level for the *Osh1Δ, Osh2Δ, Osh5Δ, Osh6Δ* deletion strains at D5 of the stationary phase (Figure 7BC).

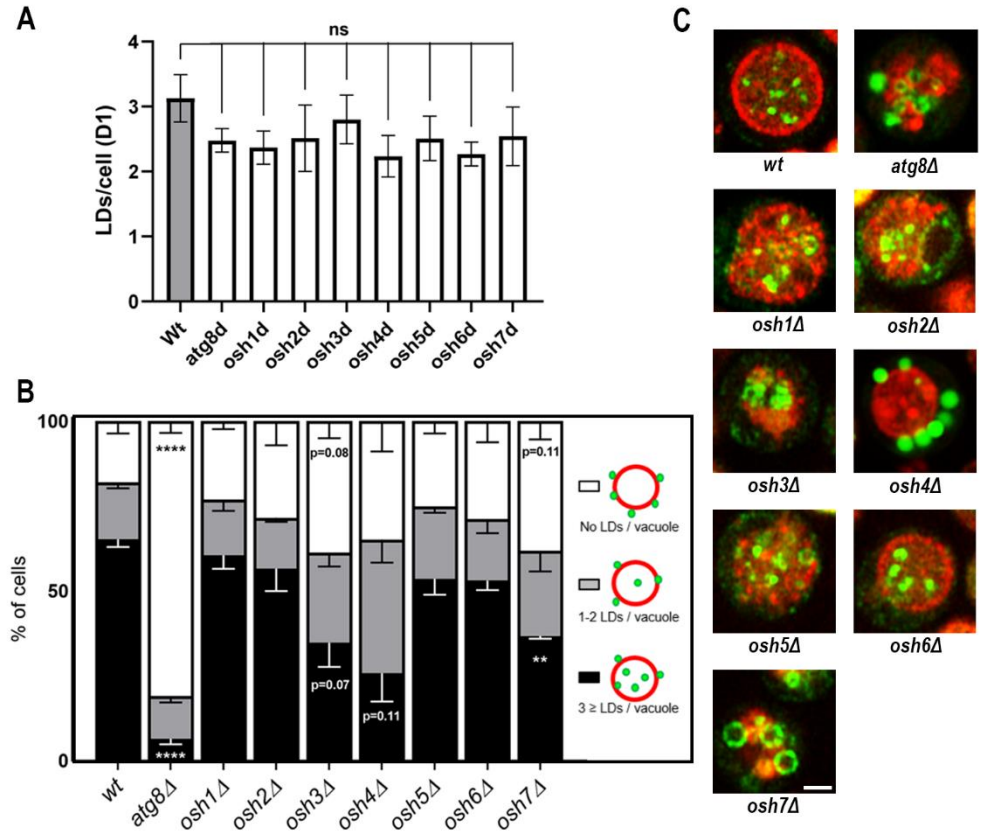

Figure 7. Several members of the OSH family show impairments in lipophagy. A) Quantification of LD number at D1 of the stationary phase in *Osh* deletion strains taken from the lipophagy library and the standard DMA (*Osh4Δ)* B) These strains were assessed for roles in stationary phase lipophagy. Quantification of lipophagy levels at the late stationary phase (D5) is shown (n=3 for *Osh4Δ,* n=4 for rest). C) Representative confocal microscopy images are shown each strain. Green fluorescent signal corresponds to LDs (BODIPY FL staining in *Osh4Δ,* Faa4-GFP in all others) and red fluorescent signal corresponds to the vacuole (FM 4-64 labelling in *Osh4Δ*, Vph1-mRuby2 in all others). Scale bar represents 2uM. Data is presented as mean of each strain with error bars showing the SEM of each experiment. Statistical testing for wild-type vs each *Osh* deletion strain by one-way ANOVA and Dunnett multiple comparisons test in A). Statistical testing in B) uses significance thresholds of **** = ($p \leq 0.0001$), *** = ($p \leq 0.001$), ** = ($p \leq 0.01$) for wild-type vs each *Osh* deletion strain by two-way ANOVA and Dunnett multiple comparisons test.

Because I observed the statistically significant involvement of Osh7 in stationary phase lipophagy and the near statistically significant involvement of Osh3 and Osh4, I was interested in assessing how these Osh proteins may be involved in the mechanism of lipophagy. As described in Chapter

1.4, a key aspect of all forms of yeast microlipophagy, including stationary phase lipophagy, is the partitioning of the vacuolar membrane into specific L_o and L_d microdomains which have distinct protein and lipid profiles. My hypothesis, as explained in Chapter 1.7, is that the Osh proteins may be involved in lipophagy by aiding in the formation or maintenance of vacuolar microdomains through their lipid transfer abilities. Therefore, I first wanted to assess whether the Osh proteins localize to the vacuole during stationary phase growth when lipophagy is becoming active and the vacuolar membrane is partitioning into microdomains. Using *S. cerevisiae* strains containing the genomic *OSH-GFP* markers from the yeast GFP collection[91] I assessed the colocalization of the Osh proteins with vacuoles labelled with FM 4-64 at D1 (Figure 8A) and D5 (Figure 8B) of the stationary phase. Notably, Osh3-GFP and Osh4-GFP show vacuolar localization at D1 of the stationary phase but prolonged growth to D5 leads to greater fluorescent intensity of these proteins and enhanced colocalization with the vacuole as observed by increased Manders colocalization coefficients (Figure 8C). The Osh7-GFP strain shows similar Manders overlap coefficients with the vacuole at both D1 and D5 of the stationary phase (Figure 8C). This data suggests that Osh3, Osh4 and Osh7 colocalize with the yeast vacuole during the stationary phase and that Osh3 and Osh4 show greater vacuolar contact as lipophagy becomes more active.

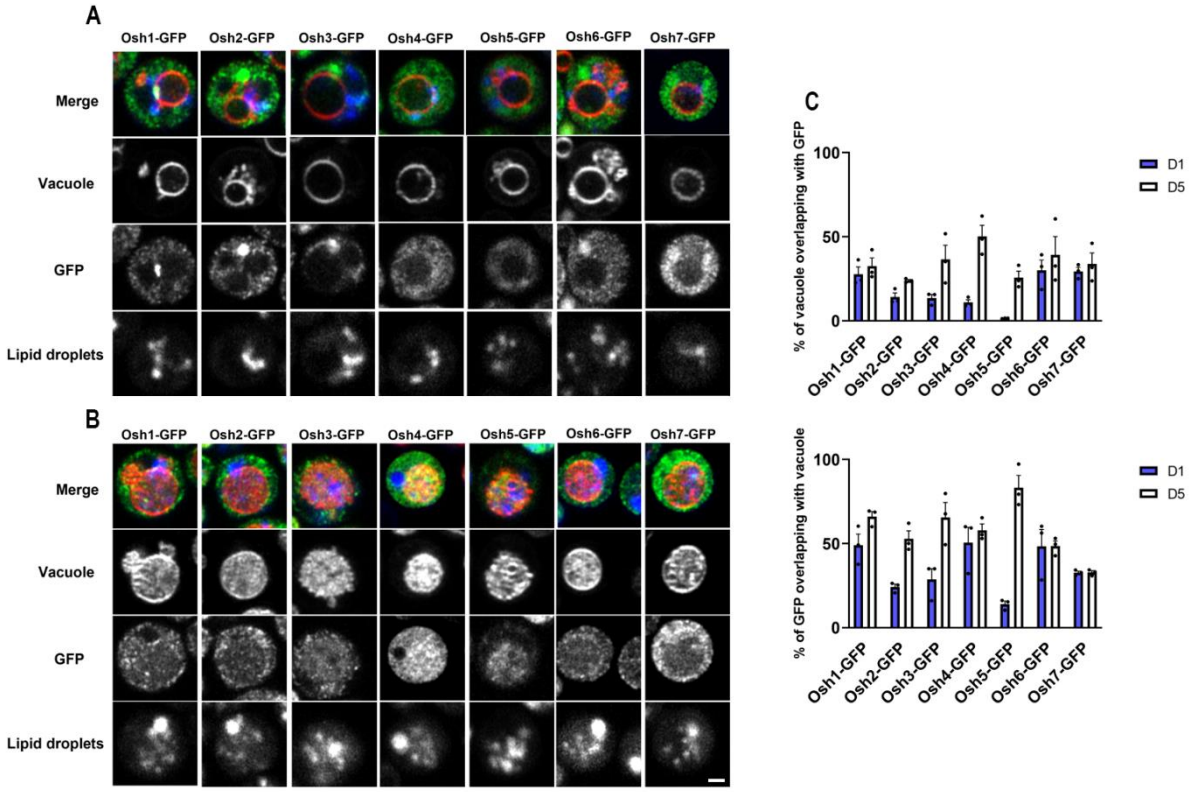

Figure 8. OSH family members localize to the vacuole during stationary phase growth. Confocal microscopy of *OSH-GFP* strains grown to D1 (A) and D5 (B) of the stationary phase. Representative confocal microscopy images are shown for each strain. Green fluorescent signal corresponds to Osh-GFP, red fluorescent signal corresponds to the vacuole (FM 4-64) and blue fluorescent signal corresponds to LDs (MDH). Scale bar represents 2uM. C) Thresholded Manders coefficients showing the percent of vacuole fluorescence overlapping with GFP fluorescence and vice-versa for each stationary phase timepoint. Data is shown as the mean coefficient of each strain with error bars showing the SEM of the image sampling.

4.1 Significance of lipophagy regulators identified via screen of yeast homologs of macrophage putative lipophagy regulators

As described, our screen of lipophagy in the yeast *S. cerevisiae* identified many regulators of yeast lipophagy. Several of the findings from this work confirmed the involvement of lipophagy regulators identified in previous works, which also highlights the validity of our lipophagy library for the identification of novel factors. I confirmed the role of *NPC2* in yeast stationary phase

lipophagy that was previously identified by Tsuji *et al.* (2017) (Figure 5A)[23]. Additionally, I identified roles in yeast stationary phase lipophagy for several yeast genes with related functions, as found through homolog/genes of similar function databases in Yeastmine and OrthoMCL 2.0b6, to the mammalian AMP-activated protein kinase (AMPK), that is involved in energy homeostasis[21]. These gene products, which were identified as positive regulators of yeast stationary phase induced lipophagy (Table 3), include: Hal5, an Snf1 related nutrient responsive kinase[92], Kkq8, a kinase paralogous to Hal5[92], Npr1, a kinase that regulates plasma membrane amino acid import[92,93] and Gal83, a subunit of the Snf1 kinase complex[94]. These observations are in line with previous findings from Seo *et al.* (2017) that two yeast homologs of AMPK, Snf1 and Snf4, have key roles in activating lipophagy during acute glucose reduction[21]. Specifically, it was found that the autophagy regulator, Atg14, interacts with Snf1 during acute glucose reduction and is trafficked from ER exit sites to the vacuolar membrane, where it assists in the formation of L_o microdomains alongside membrane-bound Atg6[21]. In the stationary phase, Atg6 and Atg14 also localize to sites of L_o microdomains and are required for lipophagy, possibly through the involvement of Snf1, though this has not been assessed before[22]. It is possible that these AMPK-related yeast genes that I identified as positive regulators of stationary phase lipophagy have similar mechanistic roles as Snf1 does in acute glucose reduction induced lipophagy, though this would need to be further investigated. I also identified a positive stationary phase induced lipophagy regulator role for Vps34 that was previously found to positively regulate lipophagy SD-N induced lipophagy[17]. It is notable that Atg6 and Atg14 are parts of Phosphatidylinositol 3 – kinase (PtdIns3-K) Complex I[95,96]. PtdIns3-K activity, mediated by Vps34 of the complex, yields PtdIns(3)P from PtdIns[95,96]. PtdIns(3)P has been observed in the cytoplasmic leaflets of the vacuolar membrane and microautophagic vesicles, as well as the luminal leaflets of

autophagosomes[23,97]. Furthermore, the presence of cellular PtdIns(3)P is required for the organized pattern of Ivy1, a marker of L_o microdomains, in the vacuolar membrane[98]. Therefore, it is possible that Vps34 has roles in stationary phase lipophagy, alongside Atg6 and Atg14, through the production and/or targeting of PtdIns(3)P to the vacuolar membrane, which may be required for microdomain partitioning. In this initial screen I also sought to confirm roles for the established positive lipophagy regulator and vacuolar lipase, Atg15, in stationary phase induced lipophagy. Intriguingly, this previous work with stationary phase induced lipophagy shows an impairment in LD-vacuolar entry following *ATG15* deletion[22]. This is possibly due to impaired L_o microdomain formation because of the reduced ability to liberate LD sterol. In contrast, my results show that *ATG15* deletion did not impair LD internalization into the vacuole in the stationary phase (Figure 5AB) but led to accumulation of vacuolar LDs, corroborating its role as a vacuolar lipase involved in LD turnover[18]. In this screen I also assessed several novel putative yeast lipophagy regulators identified through our analysis of the LD proteome in macrophages. Several of the notable lipophagy genes will be discussed here in more depth. It is also worth noting that the screening objective I took was to establish roles for putative regulators in yeast lipophagy. Therefore, any additional data on how these genes may impact LD biology, vacuolar morphology or how they may fit into the known mechanisms of yeast lipophagy is not present. However, based upon the established literature I will offer explanations for how my findings may fit into the known landscape of lipophagy in *S. cerevisiae*. Two notable yeast proteins that I identified as positive regulators of stationary phase lipophagy are Cue1, a ubiquitin binding enzyme and Ubc7, a ubiquitin conjugating enzyme (Figure 5AB). These are canonically associated with endoplasmic reticulum associated degradation (ERAD) in yeast – a process for the degradation of misfolded ER proteins that contributes to the maintenance of cellular proteostasis. These proteins being

involved in lipophagy were intriguing to us for several reasons. Firstly, in several forms of selective autophagy, including lipophagy, cargo is tagged with ubiquitin – marking it for degradation[18,40]. The finding that Cue1 and Ubc7, known regulators of ubiquitination, show strong impairments in lipophagy when genetically deleted suggested that these proteins may be ubiquitinating LD for lipophagy. Secondly, work with ER stress induced lipophagy in *S. cerevisiae* identified a role for lipophagy in the maintenance of cellular proteostasis. LDs in these yeast are associated with polyubiquitinated proteins, which are confirmed to be misfolded ER proteins that arise during ER stress with tunicamycin (TM) or dithiothreitol (DTT)[24,25]. Therefore, LDs and lipophagy regulate ER proteostasis by removing and degrading damaged proteins from the ER[24]. However, it is unclear if the LD ubiquitination is directly required for lipophagy in these conditions of ER stress. This study identified, Nup159, a nucleoporin found at the site of nuclear ER, Alg1, an ER mannosyltransferase, Tcb3, an ER membrane tethering protein and Spf1, an ER ion transporter, as proteins regulated by lipophagy-mediated proteostasis following ER stress[24]. Furthermore, ERAD components are involved with the retrotranslocation of misfolded ER proteins to the ER surface where they can be incorporated into LDs for microlipophagy mediated proteostasis[99]. It is possible that Cue1 and Ubc7 regulate this aspect of lipophagy. This highlights that these processes work in conjunction to maintain overall ER proteostasis and they additionally share certain protein targets[24,99]. Overall, while it is unclear if the proteostasis aspect of lipophagy occurs during stationary phase in the absence of an acute ER stressor, it is possible that Cue1 and Ubc7 contribute to lipophagy mediated ER proteostasis. Another possible explanation is that these ERAD components play roles in LD biology and lipophagy through regulation of the levels of Ldb16, a regulator of LD biogenesis[100]. However, other roles for these genes in the lipophagy process cannot be ruled out. Additionally, I identified Lhs1, an ER chaperone involved in protein

folding, as a positive regulator of stationary phase induced lipophagy (Figure 5AB) suggesting possible involvement of proteostasis or the transfer of ubiquitinated cargo onto LDs for this lipophagy modality. However, more work is required to determine the role of this protein. *CUE5* was another gene I assessed. As reported in Table 1. this is the yeast homolog of mammalian TOLLIP, a selective autophagy receptor involved in aggrephagy[40]. Given our lab's interest in the possible overlap of aggrephagy components with lipophagy, I was interested in assessing the role of Cue5 in stationary phase induced lipophagy in yeast. I observed similar levels of lipophagy in comparison to the wild-type strain for the *cue5Δ* strain suggesting this gene is not involved in stationary phase lipophagy (Figure 5). This finding was corroborated by another group after my work[50]. This group found that Cue5 accumulates on LDs in the stationary phase in *K. phaffii* yeast and undergoes degradation by stationary phase induced lipophagy[50]. The CUE domain of Cue5, which interacts with ubiquitin, is responsible for the binding of Cue5 to LDs[50]. However, Cue5 is dispensable for this form of *K. phaffii* lipophagy[50]. One explanation for the involvement of Cue5 in this type lipophagy is possible that it assists in the accumulation and transfer of misfolded ER protein substrates onto LDs[50]. While *K. phaffii* is a distantly related yeast to *S. cerevisiae*[101], both my findings and those of Kumar *et al.* (2022) were conducted with stationary phase induced lipophagy and show that Cue5 is dispensable for this process. Therefore, it seems possible that Cue5 may contribute to lipophagy-mediated proteostasis in *S. cerevisiae*, even if it not essential for lipophagy to function. I also identified Rnp1 as a positive regulator of lipophagy in *S. cerevisiae* (Figure 5AB). *RNP1*, which encodes a ribonucleoprotein, has been reported as homologous to mammalian Cold-inducible RNA-binding protein (CIRBP)[102], a protein highly expressed during cellular trauma and a previously reported activator of autophagy in macrophages[103,104]. In macrophages CIRBP activates autophagy through the release of reactive oxygen species[103].

However, it is unclear how Rnp1 may be involved in yeast lipophagy. Like the *atg15Δ* strain, we reported that the *ypt6Δ* strain showed no impairment in LD entry into the vacuole, but visual observations of the confocal microscopy suggest a possible impairment in vacuolar LD catabolism (Figure 5AB)[18]. Ypt6 is a GTPase involved in endosomal transport and is homologous to the mammalian GTPase, RAB6[105]. It has been reported that Ypt6 is involved in the trafficking of atg9, a key regulator of stationary phase induced lipophagy, to the PAS, where autophagosome formation begins in yeast[106]. Further work should be conducted to confirm a role for Ypt6 in yeast lipophagy and how it may regulate this process. Similarly, through this work I identified an impairment of lipophagy in the deletion strain of another yeast RAB family GTPase, *YPT31* (Figure 5AB, Table 3). Ypt31 is a known autophagy regulator in yeast[107,108]. Specifically, it has been found that inhibition of Trs130, a subunit of the transport protein particle (TRAPP) complex – a guanine exchange factor that activates Ypt31 - leads to defects in the trafficking of the core autophagy proteins, Atg8 and Atg9 to the PAS[107]. It is possible that Ypt31 regulates stationary phase induced lipophagy through the trafficking of core ATG proteins previously observed to be indispensable for lipophagy (Table 1). In mammalian cells, the Ragulator complex is a lysosomal-bound protein complex that is involved in regulating cellular metabolism. In conditions of abundant amino acids, it will activate mTOR Complex 1 (mTORCI1) for anabolic processes and will inactivate mTORC1 in conditions of low amino acids leading to AMPK activation and upregulation of catabolic processes[109]. Furthermore, through interaction with p27, the Ragulator complex can activate autophagy[110]. In *S. cerevisiae*, the EGO-TC is equivalent to the mammalian Ragulator complex[111]. Intriguingly, the EGO-TC has been observed to positively regulate yeast microautophagy[35]. Additionally, the L_o microdomain proteins, Ivy and Gtr2, interact with the EGO complex highlighting another link between this complex and microlipophagy[37]. In line with these

findings, my work identified a positive regulatory role for Ego1 and Ego2 in stationary phase induced microlipophagy in *S. cerevisiae* (Table 3). While I did not assess lipophagy roles for Ego3 nor in double or triplet genetic deletions of the EGO-TC, this work shows that Ego proteins play roles in stationary phase induced lipophagy. I observed increased vacuolar processing of Faa4-GFP into free GFP in yeast deletion strains of *TGL4* and *YPR147c* (Table 3). Both of these genes encode LD localized neutral lipases[112,113]. Tgl4 has triacylglycerol lipase, sterol hydrolase and phospholipase activity while Ypr147c has triacylglycerol lipase and fatty acid hydrolase activity[49,112]. As previously explained, it has been reported that there is crosstalk between the lipophagy and neutral lipolysis pathways in yeast[49]. My findings showing the inhibition of neutral lipolysis leading to enhanced lipophagy are in accordance with this. Furthermore, it was reported that Tgl4 is a positive regulator of acute glucose reduction induced lipophagy, which corroborates my findings[28]. I also identified Rtg1 as a positive regulator of stationary phase induced lipophagy in yeast (Table 3). I was interested in assessing this gene as through *Yeastmine* it appeared as related to mammalian TFEB, a transcription factor that activates transcription of autophagy genes, though subsequent literature analysis has shown it is actually more distantly related[114]. Rtg1, along with Rtg3, are regulators of the mitochondrial retrograde (RTG) pathway involved in maintaining mitochondrial homeostasis[115,116]. Relevant to my findings is the observation that the RTG pathway is also involved in the regulation of stationary phase mitophagy in yeast[117]. This is intriguing as other work has highlighted overlap between mitophagy and lipophagy components. Specifically, Atg32, once believed to be selectively involved in yeast mitophagy is now understood to also play roles in yeast lipophagy[21,22]. Therefore, my observations that Rtg1 positively regulates stationary phase lipophagy is in line with previous literature showing RTG involvement in stationary phase mitophagy. I also identified a role for Vps38 as a positive regulator of stationary phase lipophagy

(Table 3). Vps38 is a part of the PtdIns3-K Complex II, alongside Vps34, replacing the Atg14 found in PtdIns3-K Complex I[96,118]. Vps38 is involved in vacuolar protein sorting and endocytosis[118,119]. While a homolog of mammalian UVRAG, a known autophagy regulator, it is debated whether Vps38 is involved in yeast autophagic processes[119,120]. My observations are in support of Vps38 being a regulator of yeast lipophagy, in contrast to the findings of Van Zutphen *et al.* (2014), which did not find any involvement of Vps38 in SD-N induced lipophagy in *S. cerevisiae*[17]. However, as previously described and as shown in Table 1, there is a degree of plasticity in the genetic requirements of yeast lipophagy dependent on the induction modality used, which may explain this disparity. My observations suggest that Por2 is a negative regulator of stationary phase induced lipophagy, as indicated by enhanced Faa4-GFP cleavage in the deletion strain compared to the wild-type strain (Table 3). Por2 was identified as homolog of mammalian Voltage Dependent Anion-selective Channel 2 (VDAC2) in my analysis. VDAC2 belongs to the VDAC family of outer mitochondrial membrane ion channels and is involved in regulating mitochondrial homeostasis including bioenergetics and apoptosis[121–123]. VDAC2 also regulates mammalian autophagy[122,123]. It can promote the recruitment of the ubiquitin ligase, Parkin, for mitochondrial ubiquitination and mitophagy[123]. In contrast, another study shows that VDAC2 can also suppress autophagy through the stabilization of a complex between BECN1, an autophagy initiator and homolog of yeast Atg6, and BCL2L1[122]. In line with these multifaceted roles of VDACs in autophagy, Por1, a paralog of Por2, is a positive regulator of yeast autophagy and shows impaired autophagosome turnover in SD-N conditions upon genetic deletion[124]. Thus, Por2 may have different autophagy roles depending on the autophagic form or modality of autophagic induction. How Por2 may be involved in the regulation of stationary phase lipophagy is unclear. I also identified Yvc1 as a positive lipophagy regulator in yeast (Table 3). This gene encodes a

vacuolar cation channel that regulates Ca^{2+} release during cellular stress[125]. I was interested in assessing the role of Yvc1 in autophagy because our analysis of putative lipophagy regulators in macrophages identified Mucolipin-1 (MCOLN1), as a potential positive regulator[18]. MCOLN1 is a lysosomal cation channel belonging to the Transient receptor potential-mucolipin (TRPML) family and has been observed to activate autophagy through nuclear translocation of TFEB when stimulated[126,127]. The only yeast TRPML is Yvc1, and though there were no previously reported roles for the involvement of Yvc1 and autophagy in *S. cerevisiae,* it is possible that it may play similar roles to MCOLN1 when activated[125].

4.2 Significance of lipophagy regulators identified via further screening

Beyond this initial screen I identified other novel regulators of stationary phase lipophagy in yeast from screening of OSH family members as I was interested in them as putative lipophagy regulators due to their role in lipid trafficking as well as genes involved in aggrephagy and aggresome formation, as explained in Chapter 1.7. Additionally, I screened genes within my lipophagy library I found corresponding to GO component or function terms related to lipophagy such as autophagy, sterol transport and vacuole. This screen also included confocal microscopy validation of some strains identified as lipophagy regulators in Table 3. While much of this work shown in Figure 6 is a preliminary screen of these genes and only shows observations of n=1 for most deletion strains, it is still worthwhile to discuss the implications of my findings for these genes in yeast lipophagy. In this screen I confirmed the previously established stationary phase lipophagy roles of *YVC1, YPR147C, VPS38* and *BMH1* as shown in Table 3 (Figure 6). As with Chapter 4.1 I will discuss the significance of several of the novel lipophagy regulators I identified in this screen and offer explanations on how these observations fit into the current lipophagy body

of knowledge. This screening showed an impairment in LD internalization into the vacuole for the *lam6Δ* deletion strain during D5 of the stationary phase (Figure 6). As described, Lam6 is capable of sterol transport and has been shown to transfer ergosterol to the vacuolar membrane, and play a role in vacuolar microdomain formation, however its role in lipophagy was not previously assessed[48]. Lam6 belongs to the Lipid transfer proteins anchored at membrane contact sites (LAM) family in yeast, of which there are 6 total members[128]. The LAM family has roles in non-vesicular lipid transfer at membrane contact sites, including the ER-vacuole site[128]. These proteins are thought to specifically bind and traffic sterol via their Steroidogenic acute regulatory transfer (StART) – like domains[128,129]. Taken together, my observations suggest that Lam6 may positively regulate stationary phase lipophagy by contributing to the formation of vacuolar microdomains through the transfer of ergosterol into the vacuolar membrane[48]. As the other LAM members share functional similarity to Lam6 it would be worthwhile to assess them for lipophagy roles in the future. As observed in Table 1, many of the existing studies focused on the involvement of the core *ATG* genes in yeast lipophagy. *ATG40* is one of the more recently discovered of these genes and had not been previously assessed for lipophagy roles. Therefore, I sought to address this in my screen. Atg40 was identified as a receptor for ER-phagy in yeast[88,89]. As LD biogenesis occurs within the ER membrane, I was interested in assessing whether this ER-phagy receptor may also regulate lipophagy[7,9]. However, I did not observe any difference in lipophagy levels during the stationary phase between the *Atg40Δ* deletion strain and the wild-type (Figure 6), suggesting that this ER-phagy receptor does not overlap with lipophagy. From this screen I observed a role for Tfs1 in stationary phase induced lipophagy (Figure 6). Tfs1 is an inhibitor of carboxypeptidase Y, and was initially interesting to me as a putative stationary phase lipophagy regulator as it targets to the vacuolar membrane during the stationary phase and experiences increased expression[87]. This

suggests a possible involvement in the regulation of vacuolar microdomains and microautophagy. Intriguingly, Tfs1 has binding affinity towards PtdIns(3)P[130] which is found in the cytoplasmic leaflets of the vacuolar membrane and microautophagic vesicles[23,97]. Additionally, as explained in Chapter 4.1, PtdIns(3)P is required for the organized pattern of the L_o microdomain marker, Ivy1, within the vacuolar membrane[98]. Taken together, these findings suggest that Tfs1 may bind to PtdIns(3)P within the vacuolar membrane and regulate microdomain formation – thus contributing to lipophagy in the stationary phase. Pln1 was also identified as a positive regulator of stationary phase lipophagy in this screen (Figure 6). Pln1 is the sole yeast perilipin and is involved in the formation and stability of LDs[85]. In accordance with this I observed a lower LD number at D5 of the stationary phase for the *pln1Δ* deletion strain in comparison to the wild-type (not shown), in addition to the lipophagy impairment. This finding fits in with another study that assessed the role of LD biogenesis mediators in lipophagy. A key component of LD biology is the Fld1–Ldb16 seipin complex that stabilizes contacts between growing LDs and the ER, and is required for proper LD formation[29]. Ldb16 and an ancillary protein of this complex, Ldo16, are required for stationary phase induced lipophagy and the formation of L_o vacuolar microdomains[29]. Tracking of sterol in stationary phase grown yeast showed that it is transported from the plasma membrane to LDs before vacuolar internalization and membrane insertion by Npc2 and Ncr1[45]. This suggests that lipophagy can regulate itself through the formation of vacuolar L_o domains[22,23,45]. Therefore, Pln1 alongside Ldb16 and Ldo16 may be involved in this feedback loop by stabilizing LDs so steryl esters within the LD neutral lipid core can be incorporated into the vacuolar membrane and allow for active lipophagy. I identified Ubx3 as another positive regulator of stationary phase induced lipophagy in this screen (Figure 6). Ubx3 contains ubiquitin interacting domains and copurifies with the Dsc ubiquitin ligase complex in yeast, suggesting a close involvement with ubiquitination

processes, which as described in Chapter 4.1 are intimately involved in lipophagy[131,132]. Another possible explanation for the involvement of Ubx3 in lipophagy is that it can bind with clathrin and regulate endocytosis[90]. This is intriguing as another study identified Vps27 as a positive regulator of lipophagy in *S. cerevisiae* following diauxic shift, through its ability to bind clathrin at the site of the vacuole, which helps facilitate membrane invagination[52]. It is thought that this clathrin binding may help recruit other factors to assist in microautophagy[52]. It is possible that Ubx3 is involved in stationary phase induced lipophagy via similar means to Vps27. There are seven *UBX* genes in yeast, named for interactions with ubiquitin, and as with all identified lipophagy regulators belonging to protein families, it would be worthwhile to perform follow up lipophagy analysis on the related proteins to identify other possible genetic regulators. As described in Chapter 1.7, our group was interested in studying whether aggrephagy or aggresome related components had involvements in lipophagy. I assessed *HDA1*, the yeast homolog[64] of dHDAC6, a *Drosophila* mediator of aggresome formation shown to regulate LD degradation via the autophagy receptor p62[63]. However, I did not observe differences in lipophagy in comparison to the wild-type (Figure 6) suggesting possible differences in lipophagy regulation between these two organisms. I observed an impairment in lipophagy in the *Gvp36Δ* strain suggesting this gene may positively regulate stationary phase induced lipophagy (Figure 6). I was interested in assessing this gene as its product has been identified on the LD proteome[133], and it is has been observed to form aggregates degraded by Cue5, the selective autophagy receptor associated with aggrephagy in yeast[40]. While Cue5 is not required for lipophagy[50], as explained in Chapter 4.1, it may be involved in the transport of ubiquitinated protein onto the LD[50]. Perhaps Gvp36 is transported onto the LD by Cue5 to assist in lipophagy or simply as cargo for microlipophagy mediated proteostasis. Alternatively, Gvp36 belongs to the BAR domain superfamily of proteins, whose

Bin/Amphiphysin/Rvs167 (BAR) domains allow for binding and reshaping of membranes[67]. It has also been reported that Gvp36 has roles in in cellular adaptation to low nutrients, vacuole biogenesis and polarization of the actin cytoskeleton[68]. Each of these processes is important for stationary phase induced lipophagy, suggesting Gvp36 may be involved in lipophagy through a variety of cellular processes. The actin cytoskeleton was previously described as required for efficient SD-N induced lipophagy[23]. The *Hsp31Δ* deletion strain showed an impairment in lipophagy in comparison to the wild-type strain suggesting this gene is a positive regulator of stationary phase induced lipophagy (Figure 6). Hsp31, a homolog of mammalian PARK7, is a molecular chaperone involved in the clearance of misfolded proteins under conditions of cell stress such as nutrient limitation[86]. Furthermore, our macrophage analysis described in Chapter 3.4 identified PARK7 as a putative lipophagy regulator, which made this finding intriguing. Hsp31 has previously reported roles in stationary phase survival and autophagic activation during the stationary phase, which may explain my observations of its role in stationary phase induced lipophagy[134]. Hsp26 was also identified as positive regulator of lipophagy in this screen (Figure 6). This is a small heat shock protein with chaperone functions and is upregulated in conditions of cell stress, including heat stress and nutrient depletion also suggesting a role in cell survival[135]. Like Hsp31, Hsp26 is involved in the maintenance of protein quality under stress conditions through the sequestration of misfolded proteins where it maintains them in a near-native conformation ready to be refolded when cell stress is alleviated[69]. Hsp42 is another small heat shock protein, like Hsp26, but this genetic deletion strain did not impair lipophagy (Figure 6). Furthermore, unlike Hsp26, Hsp42 has aggregase functionality, allowing for the formation of aggregates of misfolded proteins[69]. Why the *Hsp42Δ* deletions strain was uninvolved in lipophagy is unclear. I also identified Hsp104 as a regulator of stationary phase lipophagy (Figure 6). This is

a molecular chaperone and disaggregase involved in the refolding of misfolded proteins and the clearance of aggregates[25]. Additionally, it localizes to LDs under conditions of ER stress that induce lipophagy in yeast[25]. It is intriguing that several molecular chaperones appear to be involved in lipophagy. To better understand a potential reason for this linkage it is important to understand that molecular chaperones can assist in preventing the aggregation of misfolded proteins via physical separation[69]. During stress conditions, misfolded proteins can undergo aggregation when the protein quality control mechanisms, including molecular chaperones, are overwhelmed[136]. These aggregates can accumulate into distinct inclusion bodies (IBs)[136]. Many of the aforementioned molecular chaperones including Hsp26, Hsp42 and Hsp104 colocalize with IBs, which makes sense given their roles in binding misfolded proteins[136]. Interestingly, LDs were also observed to interact with IBs and are involved in their clearance[136]. Perhaps LDs can uptake misfolded proteins from IBs like they do from the ER, as reported in Garcia *et al* (2020) and degrade them via microlipophagy[24] and perhaps these molecular chaperones are required for the targeting of LDs to IBs, and their loss impairs lipophagy. It was also shown that LDs may transfer a steryl ester derivative into IBs that could alleviate refolding stress and promote IB clearance[136]. Another possible explanation for the impaired lipophagy is that more IBs are present with the deletion of certain molecular chaperones and LDs are preferentially targeted to clear them via the steryl ester derivative, and thus are shifted away from microlipophagy mediated proteostasis. Overall, more work is required to understand this mechanism, but regardless, it is apparent that LDs and lipophagy are intimately involved in different aspects of yeast proteostasis. I identified Osh3, Osh4 and Osh7 as positive regulators of stationary phase induced lipophagy in yeast (Figure 7BC). Although the *Osh7Δ* deletion strain was the only one that reached a statistically significant impairment in lipophagy in comparison to the wild-type strain in my analysis, both the *Osh3Δ* and

*Osh4*Δ trended towards significance (Figure 7BC). Furthermore, I ruled out that these genes were impairing LD biogenesis during the stationary phase when rapid LD proliferation is induced (Figure 7A). Additionally, it appears these proteins localize to the vacuole during the stationary phase (Figure 8) with Osh3 and Osh4 increasing their level of vacuolar localization from the early to the late stationary phase. This is in line with my hypothesis that members of the OSH family of lipid trafficking proteins are involved in lipophagy via trafficking of sterol or membrane lipids onto the vacuolar membrane for the formation of microdomains. Osh proteins exchange bound lipid or sterol for membrane PtdIns(4)P[56]. The previous findings that Stt4 and Pik4 are involved in lipophagy and are required for the proper localization of PtdIns(4)Ps to the cytoplasmic leaflet of L_o vacuolar microdomains suggest that Osh3, Osh4 and Osh7 may be interacting at these sites and facilitating lipid exchange to form or maintain the microdomains[46]. However, more experimentation directly assessing the vacuolar microdomain complexity as well as the vacuolar lipidome in *Osh* mutants is required to confirm this. Previous reports indicate that Osh4-Osh7 can bind sterol, thus it is possible that Osh4 and Osh7 operate through the incorporation of yeast ergosterol into the vacuolar membrane to form L_o microdomains[55]. However, as described in Chapter 1.7, Osh7 may preferentially bind phosphatidylserine over sterol[62]. It has been described that other lipid species, including yeast sphingolipid with highly saturated acyl chains, are also involved in partitioning of the vacuolar membrane into microdomains[33,42]. It is possible the phosphatidylserine species may also be involved, as well. Finally, the identity of the lipid trafficked by Osh3 is unknown, though it is thought that its hydrophobic pocket is too small to accommodate sterol[56]. How it may regulate stationary phase induced lipophagy is unknown, but it may too be involved with the maintenance of vacuolar microdomains.

4.3 Capabilities of the lipophagy library

Herein, I developed a library of single-gene deletion strains of *S. cerevisiae* for the assessment of lipophagy. While I was unable to develop a library containing the *ERG6-Rosella* genetic marker for high-throughput lipophagy analysis, I have demonstrated that my library containing the LD marker *FAA4-GFP* and the vacuolar membrane marker *VPH1-mRuby2* is still very useful for the assessment of lipophagy via the previously validated methodologies of confocal microscopy and the *FAA4-GFP* vacuolar cleavage assay. I have identified many novel regulators of yeast lipophagy as well as validated previously discovered lipophagy genes, which highlights the accuracy and discovery power of this screen and my library. Furthermore, while my analysis solely focused on stationary phase induced lipophagy, there are other modalities of lipophagy in yeast with differing mechanisms and genetic requirements that this lipophagy library could be used in the investigation of. These include acute glucose reduction induced lipophagy or ER stress induced lipophagy with the use of ER stressors like tunicamycin or dithiothreitol. Additionally, as previously described, there is conservation of autophagic machinery between different species, and many of the initial studies of autophagy were carried out using yeast. Therefore, my lipophagy library can help provide initial insight into the genetic requirements of lipophagy in other species. It is worth noting that my library solely consists of single-gene deletions, which can be a drawback for the elucidation of lipophagy components. While I was able to identify several novel genetic regulators of yeast lipophagy using these strains, it is worth noting that there may be genetic compensation between genes that prevented certain deletion strains from showing lipophagy defects. One way to tease out these nuances in lipophagy regulators is by using strains containing multiple deletions of functionally related genes to limit compensation. While I did not perform any such analyses in this work, the lipophagy library I developed, which contains single-gene

deletions, offers an excellent starting point for the development of these multiple-deletion strains. One limitation to keep in mind regarding the lipophagy library is that due to limitations in the SGA mating technology, a small number of single-gene deletion strains of the non-essential yeast genome are not present in the current form of library. Finally, while beyond the focus of this work, the lipophagy library I developed can also be used in the widespread assessment of the genetic determinants of vacuolar morphology and LD biology under different conditions within *S. cerevisiae,* which highlights the versatility of this tool.

5.0 Conclusion

LD biology has been an active area of study in recent years and investigations into LD catabolism can lead to the development of treatment for LD related diseases like atherosclerosis and obesity. Lipophagy has emerged as an avenue for LD catabolism via lipolysis within the acidic lysosome or vacuole. I sought to better understand the genetic regulation of lipophagy within budding yeast, *S. cerevisiae*, an organism often used for the study of autophagic processes. To do this I developed a lipophagy library containing LD and vacuole fluorescent protein markers and single gene deletions of the entire yeast non-essential genome. I have demonstrated the ability of this library to assess lipophagy and identified multiple novel regulators of stationary phase lipophagy in yeast. While I did not provide any experimental mechanistic insight into how these genes regulate lipophagy, the sheer number of genes tested and identified as being involved in lipophagy highlights the power and significance of my library. Additionally, there are multiple modalities of yeast lipophagy, each induced by different conditions, and each with varying genetic requirements. My library can be used to assess lipophagy for each of these modalities beyond the stationary phase induced lipophagy I investigated. In conclusion, I have developed a powerful tool for the determination of the genetics of lipophagy in *S. cerevisiae*, and there is much more to be discovered from my lipophagy library beyond the findings presented herein.

6.0 Contribution of collaborators

Dr. Sylvain Huard assisted in the construction of the lipophagy query strains for the SGA mating, by developing the *ERG6-Rosella* query strain as well as adding the *FAA4-GFP* marker into Y7092 query background. Viyashini Vijithakumar, a Masters student in the lab of Dr. Mireille Ouimet conducted the immunoblots for the Faa4-GFP vacuolar cleavage assays in Table 3.

7.0 References

1. Parzych, K. R. & Klionsky, D. J. An Overview of Autophagy: Morphology, Mechanism, and Regulation. *Antioxid. Redox Signal.* **20**, 460 (2014).
2. Lamming, D. W. & Bar-Peled, L. Lysosome: The Metabolic Signaling Hub. *Traffic* **20**, 27 (2019).
3. Feng, Y., He, D., Yao, Z. & Klionsky, D. J. The machinery of macroautophagy. *Cell Res. 2014 241* **24**, 24–41 (2013).
4. Schuck, S. Microautophagy – distinct molecular mechanisms handle cargoes of many sizes. (2020) doi:10.1242/jcs.246322.
5. Kaushik, S. & Maria Cuervo, A. The coming of age of chaperone-mediated autophagy. (2018) doi:10.1038/s41580-018-0001-6.
6. Tekirdag, K. & Cuervo, A. M. Chaperone-mediated autophagy and endosomal microautophagy: Jointed by a chaperone. *J. Biol. Chem.* **293**, 5414 (2018).
7. Onal, G., Kutlu, O., Gozuacik, D. & Dokmeci Emre, S. Lipid Droplets in Health and Disease. *Lipids in Health and Disease* (2017) doi:10.1186/s12944-017-0521-7.
8. Boucher, D., Vijithakumar, V. & Ouimet, M. Lipid Droplets as Regulators of Metabolism and Immunity. *Immunometabolism* (2021) doi:10.20900/immunometab20210021.
9. Olzmann, J. A. & Carvalho, P. Dynamics and functions of lipid droplets. *Nat. Rev. Mol. Cell Biol. 2018 203* **20**, 137–155 (2018).
10. Jarc, E. & Petan, T. A twist of FATe: Lipid droplets and inflammatory lipid mediators. *Biochimie* **169**, 69–87 (2020).
11. Walther, T. C. & Farese, R. V. Lipid Droplets And Cellular Lipid Metabolism. *Annu. Rev. Biochem.* **81**, 687 (2012).
12. Guerrini, V. & Gennaro, M. L. Foam cells: one size doesn't fit all. *Trends Immunol.* **40**, 1163 (2019).
13. Singh, R. *et al.* Autophagy regulates lipid metabolism. *Nature* (2009) doi:10.1038/nature07976.
14. Ouimet, M. *et al.* Autophagy regulates cholesterol efflux from macrophage foam cells via lysosomal acid lipase. *Cell Metab.* (2011) doi:10.1016/j.cmet.2011.03.023.
15. Jung, W. *et al.* Lipophagy prevents activity-dependent neurodegeneration due to dihydroceramide accumulation in vivo . *EMBO Rep.* **18**, 1150–1165 (2017).
16. Zienkiewicz, K. & Zienkiewicz, A. Degradation of Lipid Droplets in Plants and Algae—Right Time, Many Paths, One Goal. *Front. Plant Sci.* **11**, 1–14 (2020).
17. Van Zutphen, T. *et al.* Lipid droplet autophagy in the yeast Saccharomyces cerevisiae. *Mol. Biol. Cell* (2014) doi:10.1091/mbc.E13-08-0448.

18. Robichaud, S. *et al.* Identification of novel lipid droplet factors that regulate lipophagy and cholesterol efflux in macrophage foam cells. *Autophagy* **00**, 1–19 (2021).

19. Chen, K., Yuan, R., Zhang, Y., Geng, S. & Li, L. Tollip Deficiency Alters Atherosclerosis and Steatosis by Disrupting Lipophagy. *J. Am. Heart Assoc.* **6**, (2017).

20. Schulze, R. J. *et al.* Direct lysosome-based autophagy of lipid droplets in hepatocytes. *Proc. Natl. Acad. Sci. U. S. A.* **117**, 32443–32452 (2020).

21. Seo, A. Y. *et al.* AMPK and vacuole-associated Atg14p orchestrate μ-lipophagy for energy production and long-term survival under glucose starvation. *Elife* (2017) doi:10.7554/eLife.21690.

22. Wang, C. W., Miao, Y. H. & Chang, Y. S. A sterol-enriched vacuolar microdomain mediates stationary phase lipophagy in budding yeast. *J. Cell Biol.* (2014) doi:10.1083/jcb.201404115.

23. Tsuji, T. *et al.* Niemann-Pick type C proteins promote microautophagy by expanding raft-like membrane domains in the yeast vacuole. *Elife* (2017) doi:10.7554/eLife.25960.

24. Garcia, E. J. *et al.* Membrane dynamics and protein targets of lipid droplet microautophagy during ER stress-induced proteostasis in the budding yeast, Saccharomyces cerevisiae. *Autophagy* 1–21 (2020) doi:10.1080/15548627.2020.1826691.

25. Vevea, J. D. *et al.* Role for Lipid Droplet Biogenesis and Microlipophagy in Adaptation to Lipid Imbalance in Yeast. *Dev. Cell* (2015) doi:10.1016/j.devcel.2015.11.010.

26. Kumar, R., Rahman, M. A. & Nazarko, T. Y. Nitrogen starvation and stationary phase lipophagy have distinct molecular mechanisms. *Int. J. Mol. Sci.* **21**, 1–14 (2020).

27. Liao, P. C., Garcia, E. J., Tan, G., Tsang, C. A. & Pon, L. A. Roles for L o microdomains and ESCRT in ER stress-induced lipid droplet microautophagy in budding yeast. *Mol. Biol. Cell* **32**, br12 (2021).

28. Zhang, A., Meng, Y., Li, Q. & Liang, Y. The endosomal sorting complex required for transport complex negatively regulates Erg6 degradation under specific glucose restriction conditions. *Traffic* (2020) doi:10.1111/tra.12732.

29. Teixeira, V. *et al.* Regulation of lipid droplets by metabolically controlled Ldo isoforms. *J. Cell Biol.* (2018) doi:10.1083/jcb.201704115.

30. Werner-Washburne, M., Braun, E., Johnston, G. C. & Singer, R. A. Stationary phase in the yeast Saccharomyces cerevisiae. *Microbiol. Rev.* **57**, 383–401 (1993).

31. Nguyen, T. B. *et al.* DGAT1-dependent lipid droplet biogenesis protects mitochondrialfunction during starvation-induced autophagy. *Dev. Cell* **42**, 9 (2017).

32. Aris, J. P. *et al.* Respiration Proficiency During Calorie Restriction in Yeast. **48**, 1107–1119 (2014).

33. Toulmay, A. & Prinz, W. A. Direct imaging reveals stable, micrometer-scale lipid domains that segregate proteins in live cells. *J. Cell Biol.* (2013) doi:10.1083/jcb.201301039.

34. Hurst, L. R. & Fratti, R. A. Lipid Rafts, Sphingolipids, and Ergosterol in Yeast Vacuole Fusion and Maturation. *Front. Cell Dev. Biol.* **8**, 1–7 (2020).

35. Dubouloz, F., Deloche, O., Wanke, V., Cameroni, E. & De Virgilio, C. The TOR and EGO protein complexes orchestrate microautophagy in yeast. *Mol. Cell* **19**, 15–26 (2005).

36. Yoshii, S. R. & Mizushima, N. Monitoring and measuring autophagy. *Int. J. Mol. Sci.* **18**, 1–13 (2017).

37. Varlakhanova, N. V., Tornabene, B. A. & Ford, M. G. J. Ivy1 is a negative regulator of Gtr-dependent TORC1 activation. *J. Cell Sci.* **131**, (2018).

38. Peselj, C. *et al.* Sterol Metabolism Differentially Contributes to Maintenance and Exit of Quiescence. *Front. Cell Dev. Biol.* **10**, 187 (2022).

39. Noda, N. N. & Fujioka, Y. Atg1 family kinases in autophagy initiation. *Cell. Mol. Life Sci.* **72**, (2015).

40. Farré, J. C. & Subramani, S. Mechanistic insights into selective autophagy pathways: Lessons from yeast. *Nat. Rev. Mol. Cell Biol.* **17**, 537–552 (2016).

41. Teter, S. A. *et al.* Degradation of lipid vesicles in the yeast vacuole requires function of Cvt17, a putative lipase. *J. Biol. Chem.* **276**, 2083–2087 (2001).

42. Klose, C. *et al.* Yeast Lipids Can Phase-separate into Micrometer-scale Membrane Domains. *J. Biol. Chem.* **285**, 30224 (2010).

43. Schlarmann, P., Ikeda, A. & Funato, K. Membrane contact sites in yeast: Control hubs of sphingolipid homeostasis. *Membranes (Basel).* **11**, (2021).

44. Yamagata, M., Obara, K. & Kihara, A. Sphingolipid synthesis is involved in autophagy in Saccharomyces cerevisiae. *Biochem. Biophys. Res. Commun.* **410**, 786–791 (2011).

45. Winkler, M. B. L. *et al.* Structural Insight into Eukaryotic Sterol Transport through Niemann-Pick Type C Proteins. *Cell* **179**, 485-497.e18 (2019).

46. Kurokawa, Y. *et al.* Microautophagy in the yeast vacuole depends on the activities of phosphatidylinositol 4-kinases, Stt4p and Pik1p. *Biochim. Biophys. Acta - Biomembr.* **1862**, 183416 (2020).

47. Tomioku, K. na *et al.* Nanoscale domain formation of phosphatidylinositol 4-phosphate in the plasma and vacuolar membranes of living yeast cells. *Eur. J. Cell Biol.* **97**, 269–278 (2018).

48. Murley, A. *et al.* Ltc1 is an ER-localized sterol transporter and a component of ER-mitochondria and ER-vacuole contacts. *J. Cell Biol.* **209**, 539–548 (2015).

49. Maeda, Y., Oku, M. & Sakai, Y. A defect of the vacuolar putative lipase Atg15 accelerates degradation of lipid droplets through lipolysis. *Autophagy* **11**, 1247–1258 (2015).

50. Kumar, R., Shroff, A. & Nazarko, T. Y. Komagataella phaffii Cue5 Piggybacks on Lipid Droplets for Its Vacuolar Degradation during Stationary Phase Lipophagy. *Cells* **11**, 1–13

(2022).

51. Barbosa, A. D. & Siniossoglou, S. Spatial distribution of lipid droplets during starvation: Implications for lipophagy. *Commun. Integr. Biol.* **9**, 1–4 (2016).

52. Oku, M. *et al.* Evidence for ESC RT- and clathrin-dependent microautophagy. *J. Cell Biol.* (2017) doi:10.1083/jcb.201611029.

53. Nakatogawa, H., Suzuki, K., Kamada, Y. & Ohsumi, Y. Dynamics and diversity in autophagy mechanisms: lessons from yeast. *Nat. Rev. Mol. Cell Biol. 2009 107* **10**, 458–467 (2009).

54. Kanki, T. *et al.* A genomic screen for yeast mutants defective in selective mitochondria autophagy. *Mol. Biol. Cell* (2009) doi:10.1091/mbc.E09-03-0225.

55. Tian, S., Ohta, A., Horiuchi, H. & Fukuda, R. Oxysterol-binding protein homologs mediate sterol transport from the endoplasmic reticulum to mitochondria in yeast. *J. Biol. Chem.* **293**, 5636 (2018).

56. Tong, J., Manik, M. K., Yang, H. & Im, Y. J. Structural insights into nonvesicular lipid transport by the oxysterol binding protein homologue family. *Biochim. Biophys. Acta - Mol. Cell Biol. Lipids* **1861**, 928–939 (2016).

57. Sokolov, S. S., Trushina, N. I., Severin, F. F. & Knorre, D. A. Ergosterol Turnover in Yeast: An Interplay between Biosynthesis and Transport. *Biochem. 2019 844* **84**, 346–357 (2019).

58. Im, Y. J., Raychaudhuri, S., Prinz, W. A. & Hurley, J. H. Structural mechanism for sterol sensing and transport by OSBP-related proteins. *Nat. 2005 4377055* **437**, 154–158 (2005).

59. Von Filseck, J. M., Vanni, S., Mesmin, B., Antonny, B. & Drin, G. A phosphatidylinositol-4-phosphate powered exchange mechanism to create a lipid gradient between membranes. *Nat. Commun. 2015 61* **6**, 1–12 (2015).

60. Mesmin, B. & Antonny, B. The counterflow transport of sterols and PI4P. *Biochim. Biophys. Acta - Mol. Cell Biol. Lipids* **1861**, 940–951 (2016).

61. de Saint-Jean, M. *et al.* Osh4p exchanges sterols for phosphatidylinositol 4-phosphate between lipid bilayers. *J. Cell Biol.* **195**, 965–978 (2011).

62. Maeda, K. *et al.* Interactome map uncovers phosphatidylserine transport by oxysterol-binding proteins. *Nature* **501**, 257–261 (2013).

63. Yan, Y. *et al.* HDAC6 regulates lipid droplet turnover in response to nutrient deprivation via p62-mediated selective autophagy. *J. Genet. Genomics* (2019) doi:10.1016/j.jgg.2019.03.008.

64. Zhang, M. *et al.* HDAC6 regulates DNA damage response via deacetylating MLH1. *J. Biol. Chem.* **294**, 5813 (2019).

65. Wang, Y. *et al.* Abnormal proteins can form aggresome in yeast: aggresome-targeting signals and components of the machinery. *FASEB J.* **23**, 451 (2009).

66. Xu, Z. *et al.* 14-3-3 protein targets misfolded chaperone-associated proteins to aggresomes. *J. Cell Sci.* **126**, 4173–4186 (2013).

67. Prigent, M., Chaillot, J., Tisserand, H., Boy-Marcotte, E. & Cuif, M. H. Three members of the yeast N-BAR proteins family form heterogeneous lattices in vivo and interact differentially with two RabGAP proteins. *Sci. Reports 2020 101* **10**, 1–14 (2020).

68. Querin, L. *et al.* Proteomic analysis of a nutritional shift-up in Saccharomyces cerevisiae identifies Gvp36 as a BAR-containing protein involved in vesicular traffic and nutritional adaptation. *J. Biol. Chem.* **283**, 4730–4743 (2008).

69. Ungelenk, S. *et al.* Small heat shock proteins sequester misfolding proteins in near-native conformation for cellular protection and efficient refolding. *Nat. Commun.* **7**, (2016).

70. Kumar, A., Mathew, V. & Stirling, P. C. Nuclear protein quality control in yeast: The latest INQuiries. *J. Biol. Chem.* **298**, 102199 (2022).

71. Malinovska, L., Kroschwald, S., Munder, M. C., Richter, D. & Alberti, S. Molecular chaperones and stress-inducible protein-sorting factors coordinate the spatiotemporal distribution of protein aggregates. *Mol. Biol. Cell* **23**, 3041 (2012).

72. Longtine, M. S. *et al.* Additional modules for versatile and economical PCR-based gene deletion and modification in Saccharomyces cerevisiae. *Yeast* (1998) doi:10.1002/(SICI)1097-0061(199807)14:10<953::AID-YEA293>3.0.CO;2-U.

73. Baryshnikova, A. *et al.* Synthetic Genetic Array (SGA) Analysis in Saccharomyces cerevisiae and Schizosaccharomyces pombe. *Methods Enzymol.* **470**, 145–179 (2010).

74. Tong, A. H. Y. *et al.* Systematic genetic analysis with ordered arrays of yeast deletion mutants. *Science (80-.).* (2001) doi:10.1126/science.1065810.

75. Tong, A. H. Y. & Boone, C. Synthetic genetic array analysis in Saccharomyces cerevisiae. *Methods Mol. Biol.* **313**, 171–192 (2006).

76. Rosado, C. J., Mijaljica, D., Hatzinisiriou, I., Prescott, M. & Devenish, R. J. Rosella: A fluorescent pH-biosensor for reporting vacuolar turnover of cytosol and organelles in yeast. *Autophagy* (2008) doi:10.4161/auto.5331.

77. Mijaljica, D., Prescott, M. & Devenish, R. J. A Late Form of Nucleophagy in Saccharomyces cerevisiae. *PLoS One* **7**, 40013 (2012).

78. Mijaljica, D., Prescott, M. & Devenish, R. J. A Fluorescence Microscopy Assay for Monitoring Mitophagy in the Yeast Saccharomyces cerevisiae. *J. Vis. Exp.* **53**, (2011).

79. Miesenböck, G., De Angelis, D. A. & Rothman, J. E. Visualizing secretion and synaptic transmission with pH-sensitive green fluorescent proteins. *Nature* **394**, 192–195 (1998).

80. Diakov, T. T., Tarsio, M. & Kane, P. M. Measurement of Vacuolar and Cytosolic pH In Vivo in Yeast Cell Suspensions. *J. Vis. Exp.* 50261 (2013) doi:10.3791/50261.

81. Hanson, S. J. & Wolfe, K. H. An Evolutionary Perspective on Yeast Mating-Type Switching. *Genetics* **206**, 9 (2017).

82. Neiman, A. M. Sporulation in the Budding Yeast Saccharomyces cerevisiae. *Genetics* **189**, 737 (2011).

83. Torggler, R., Papinski, D. & Kraft, C. Assays to Monitor Autophagy in Saccharomyces cerevisiae. *Cells* **6**, 23 (2017).

84. Klionsky, D. J. *et al.* Guidelines for the use and interpretation of assays for monitoring autophagy (3rd edition). *Autophagy* **12**, 1 (2016).

85. Gao, Q. *et al.* Pet10p is a yeast perilipin that stabilizes lipid droplets and promotes their assembly. *J. Cell Biol.* (2017) doi:10.1083/jcb.201610013.

86. Aslam, K. & Hazbun, T. R. Hsp31, a member of the DJ-1 superfamily, is a multitasking stress responder with chaperone activity. *Prion* (2016) doi:10.1080/19336896.2016.1141858.

87. Fukada, H., Mima, J., Nagayama, M., Kato, M. & Ueda, M. Biochemical Analysis of the Yeast Proteinase Inhibitor (I C) Homolog I C h and Its Comparison with I C. doi:10.1271/bbb.60528.

88. Mochida, K. *et al.* Receptor-mediated selective autophagy degrades the endoplasmic reticulum and the nucleus. *Nature* **522**, 359–362 (2015).

89. Cui, Y. *et al.* A COPII subunit acts with an autophagy receptor to target endoplasmic reticulum for degradation. *Science* **365**, 53 (2019).

90. Farrell, K. B., Grossman, C. & Di Pietro, S. M. New regulators of clathrin-mediated endocytosis identified in saccharomyces cerevisiae by systematic quantitative fluorescence microscopy. *Genetics* **201**, 1061–1070 (2015).

91. Huh, W. K. *et al.* Global analysis of protein localization in budding yeast. *Nature* (2003) doi:10.1038/nature02026.

92. Tumolo, J. M., Hepowit, N. L., Joshi, S. S. & MacGurn, J. A. A Snf1-related nutrient-responsive kinase antagonizes endocytosis in yeast. *PLOS Genet.* **16**, e1008677 (2020).

93. De Craene, J. O., Soetens, O. & André, B. The Npr1 Kinase Controls Biosynthetic and Endocytic Sorting of the Yeast Gap1 Permease. *J. Biol. Chem.* **276**, 43939–43948 (2001).

94. Hedbacker, K. & Carlson, M. Regulation of the nucleocytoplasmic distribution of Snf1-Gal83 protein kinase. *Eukaryot. Cell* **5**, 1950–1956 (2006).

95. Obara, K. & Ohsumi, Y. Atg14: A key player in orchestrating autophagy. *Int. J. Cell Biol.* **2011**, (2011).

96. Lrincz, P. *et al.* Atg6/UVRAG/Vps34-Containing Lipid Kinase Complex Is Required for Receptor Downregulation through Endolysosomal Degradation and Epithelial Polarity during Drosophila Wing Development. *Biomed Res. Int.* **2014**, (2014).

97. Cheng, J. *et al.* Yeast and mammalian autophagosomes exhibit distinct phosphatidylinositol 3-phosphate asymmetries. *Nat. Commun. 2014 51* **5**, 1–12 (2014).

98. Numrich, J. *et al.* The I-BAR protein Ivy1 is an effector of the Rab7 GTPase Ypt7

involved in vacuole membrane homeostasis. *J. Cell Sci.* **128**, 2278–2292 (2015).

99. Brodsky, J. L. Cleaning Up: ER-Associated Degradation to the Rescue. *Cell* **151**, 1163–1167 (2012).

100. Wang, C. W., Miao, Y. H. & Chang, Y. S. Control of lipid droplet size in budding yeast requires the collaboration between Fld1 and Ldb16. *J. Cell Sci.* **127**, 1214–1228 (2014).

101. Bernauer, L., Radkohl, A., Lehmayer, L. G. K. & Emmerstorfer-Augustin, A. Komagataella phaffii as Emerging Model Organism in Fundamental Research. *Front. Microbiol.* **11**, 3462 (2021).

102. Doi, A. *et al.* Chemical genomics approach to identify genes associated with sensitivity to rapamycin in the fission yeast Schizosaccharomyces pombe. *Genes to Cells* **20**, 292–309 (2015).

103. Li, Z. *et al.* Cold-inducible RNA-binding protein through TLR4 signaling induces mitochondrial DNA fragmentation and regulates macrophage cell death after trauma. *Cell Death Dis. 2017 85* **8**, e2775–e2775 (2017).

104. Qiang, X. *et al.* Cold-inducible RNA-binding protein (CIRP) triggers inflammatory responses in hemorrhagic shock and sepsis. *Nat. Med. 2013 1911* **19**, 1489–1495 (2013).

105. Li, B. & Warner, J. R. Mutation of the Rab6 homologue of Saccharomyces cerevisiae, YPT6, inhibits both early Golgi function and ribosome biosynthesis. *J. Biol. Chem.* **271**, 16813–16819 (1996).

106. Yang, S. & Rosenwald, A. G. Autophagy in Saccharomyces cerevisiae requires the monomeric GTP-binding proteins, Arl1 and Ypt6. *Autophagy* **12**, 1721 (2016).

107. Zou, S. *et al.* Trs130 participates in autophagy through GTPases Ypt31/32 in Saccharomyces cerevisiae. *Traffic* **14**, 233 (2013).

108. Kramer, M. H. *et al.* Molecular Cell Resource Active Interaction Mapping Reveals the Hierarchical Organization of Autophagy. *Mol. Cell* **65**, 761–774 (2017).

109. Colaço, A. & Jäättelä, M. Ragulator—a multifaceted regulator of lysosomal signaling and trafficking. *J. Cell Biol.* **216**, 3895 (2017).

110. Nowosad, A. *et al.* p27 controls Ragulator and mTOR activity in amino acid-deprived cells to regulate the autophagy-lysosomal pathway and coordinate cell cycle and cell growth. *Nat. Cell Biol.* **22**, 1076–1090 (2020).

111. Zhang, T. *et al.* Structural insights into the EGO-TC–mediated membrane tethering of the TORC1-regulatory Rag GTPases. *Sci. Adv.* **5**, (2019).

112. Naresh Kumar, M., Thunuguntla, V. B. S. C., Chandra Sekhar, B. & Bondili, J. S. Saccharomyces cerevisiae lipid droplet associated enzyme Ypr147cp shows both TAG lipase and ester hydrolase activities. *J. Gen. Appl. Microbiol.* **64**, 76–83 (2018).

113. Athenstaedt, K. & Nther Daum, G. Tgl4p and Tgl5p, Two Triacylglycerol Lipases of the Yeast Saccharomyces cerevisiae Are Localized to Lipid Particles *. *J. Biol. Chem.* **280**, 37301–37309 (2005).

114. Taniguchi, M. *et al.* TFE3 Is a bHLH-ZIP-type Transcription Factor that Regulates the Mammalian Golgi Stress Response. *Cell Struct. Funct.* **40**, 13–30 (2015).

115. Ruiz-Roig, C., Noriega, N., Duch, A., Posas, F. & De Nadal, E. The Hog1 SAPK controls the Rtg1/Rtg3 transcriptional complex activity by multiple regulatory mechanisms. *Mol. Biol. Cell* **23**, 4286 (2012).

116. Hashim, Z., Mukai, Y., Bamba, T. & Fukusaki, E. Metabolic Profiling of Retrograde Pathway Transcription Factors Rtg1 and Rtg3 Knockout Yeast. *Metabolites* **4**, 580 (2014).

117. Journo, D., Mor, A. & Abeliovich, H. Aup1-mediated Regulation of Rtg3 during Mitophagy. *J. Biol. Chem.* **284**, 35885 (2009).

118. Lee, H. N. *et al.* Vacuolar Trafficking Protein VPS38 Is Dispensable for Autophagy. *Plant Physiol.* **176**, 1559 (2018).

119. Levine, B., Liu, R., Dong, X. & Zhong, Q. Beclin orthologs: integrative hubs of cell signaling, membrane trafficking, and physiology. *Trends Cell Biol.* **25**, 533 (2015).

120. Song, Y., Quach, C. & Liang, C. UVRAG in autophagy, inflammation, and cancer. *Autophagy* **16**, 387–388 (2020).

121. Naghdi, S. & Hajnóczky, G. VDAC2-specific cellular functions and the underlying structure. *Biochim. Biophys. Acta - Mol. Cell Res.* **1863**, 2503–2514 (2016).

122. Yuan, J. *et al.* MYBL2 guides autophagy suppressor VDAC2 in the developing ovary to inhibit autophagy through a complex of VDAC2-BECN1-BCL2L1 in mammals. *Autophagy* **11**, 1081 (2015).

123. Sun, Y., Vashisht, A. A., Tchieu, J., Wohlschlegel, J. A. & Dreier, L. Voltage-dependent Anion Channels (VDACs) Recruit Parkin to Defective Mitochondria to Promote Mitochondrial Autophagy. *J. Biol. Chem.* **287**, 40652 (2012).

124. Broeskamp, F. *et al.* Porin 1 modulates autophagy in yeast. *Cells* **10**, (2021).

125. Venkatachalam, K., Wong, C. O. & Zhu, M. X. The role of TRPMLs in endolysosomal trafficking and function. *Cell Calcium* (2015) doi:10.1016/j.ceca.2014.10.008.

126. Zhang, X. *et al.* MCOLN1 is a ROS sensor in lysosomes that regulates autophagy. *Nat. Commun.* (2016) doi:10.1038/ncomms12109.

127. Tedeschi, V. *et al.* The activation of Mucolipin TRP channel 1 (TRPML1) protects motor neurons from L-BMAA neurotoxicity by promoting autophagic clearance. *Sci. Reports 2019 91* **9**, 1–11 (2019).

128. Tong, J., Manik, M. K. & Im, Y. J. Structural basis of sterol recognition and nonvesicular transport by lipid transfer proteins anchored at membrane contact sites. *Proc. Natl. Acad. Sci. U. S. A.* **115**, E856–E865 (2018).

129. Gatta, A. T. *et al.* A new family of StART domain proteins at membrane contact sites has a role in ER-PM sterol transport. *Elife* **4**, 1–46 (2015).

130. Mima, J., Fukada, H., Nagayama, M. & Ueda, M. Specific membrane binding of the

carboxypeptidase Y inhibitor IC, a phosphatidylethanolamine-binding protein family member. *FEBS J.* **273**, 5374–5383 (2006).

131. Hartmann-Petersen, R. *et al.* The Ubx2 and Ubx3 cofactors direct Cdc48 activity to proteolytic and nonproteolytic ubiquitin-dependent processes. *Curr. Biol.* **14**, 824–828 (2004).

132. Yang, X., Arines, F. M., Zhang, W. & Li, M. Sorting of a multi-subunit ubiquitin ligase complex in the endolysosome system. *Elife* **7**, (2018).

133. Grillitsch, K. *et al.* Lipid particles/droplets of the yeast Saccharomyces cerevisiae revisited: Lipidome meets Proteome. *Biochim. Biophys. Acta - Mol. Cell Biol. Lipids* (2011) doi:10.1016/j.bbalip.2011.07.015.

134. Miller-Fleming, L. *et al.* Yeast DJ-1 superfamily members are required for diauxic-shift reprogramming and cell survival in stationary phase. *Proc. Natl. Acad. Sci. U. S. A.* (2014) doi:10.1073/pnas.1319221111.

135. Campion, R. *et al.* Proteomic analysis of dietary restriction in yeast reveals a role for Hsp26 in replicative lifespan extension. *Biochem. J.* **478**, 4153 (2021).

136. Moldavski, O. *et al.* Lipid Droplets Are Essential for Efficient Clearance of Cytosolic Inclusion Bodies. *Dev. Cell* **33**, 603–610 (2015).

137. Ba Hler, J. R. *et al.* Heterologous Modules for Efficient and Versatile PCR-based Gene Targeting in Schizosaccharomyces pombe. doi:10.1002/(SICI)1097-0061(199807)14:10.

138. Van Driessche, B., Tafforeau, L., Hentges, P., Carr, A. M. & Vandenhaute, J. Additional vectors for PCR-based gene tagging in Saccharomyces cerevisiae and Schizosaccharomyces pombe using nourseothricin resistance. *Yeast* **22**, 1061–1068 (2005).

139. Lee, S., Lim, W. A. & Thorn, K. S. Improved Blue, Green, and Red Fluorescent Protein Tagging Vectors for S. cerevisiae. *PLoS One* **8**, 67902 (2013).

8.0 Appendix

Table S1. Strain list

Strain name	Genotype	Source
Y7092 (SGA query strain)	***MATα*** *can1Δ::STE2pr-SP-his5 lyp1Δ his3Δ1 leu2Δ0 ura3Δ0 met15Δ0 LYS2+*	SGA Starter Kit[73]
YKB4890 Lipophagy query strain *(Y7092)*	*(Y7092) FAA4-GFP::NatMX6 VPH1-mRuby2::Hph*	This Study *Y7092* background[73]
atg8Δ (developed by PCR method[72])	*(YKB4890) atg8Δ::KanMX4*	This Study
atg8Δ	*(YKB4890) atg8Δ::KanMX4*	This Study (Lipophagy library)
lhs1Δ	*(YKB4890) lhs1Δ::KanMX4*	This Study (Lipophagy library)
rnp1Δ	*(YKB4890) rnp1Δ::KanMX4*	This Study (Lipophagy library)
ubc7Δ	*(YKB4890) ubc7Δ::KanMX4*	This Study (Lipophagy library)
cue1Δ	*(YKB4890) cue1Δ::KanMX4*	This Study (Lipophagy library)
ypt6Δ	*(YKB4890) ypt6Δ::KanMX4*	This Study (Lipophagy library)
ypt31Δ	*(YKB4890) ypt31Δ::KanMX4*	This Study (Lipophagy library)
atg15Δ	*(YKB4890) atg15Δ::KanMX4*	This Study (Lipophagy library)
hsp82Δ	*(YKB4890) hsp82Δ::KanMX4*	This Study (Lipophagy library)
ssa3Δ	*(YKB4890) ssa3Δ::KanMX4*	This Study (Lipophagy library)
cue5Δ	*(YKB4890) cue5Δ::KanMX4*	This Study (Lipophagy library)
npc2Δ	*(YKB4890) npc2Δ::KanMX4*	This Study (Lipophagy library)
atg9Δ	*(YKB4890) atg9Δ::KanMX4*	This Study (Lipophagy library)
atg32Δ	*(YKB4890) atg32Δ::KanMX4*	This Study (Lipophagy library)
atg21Δ	*(YKB4890) atg21Δ::KanMX4*	This Study (Lipophagy library)

vps34Δ	*(YKB4890)*	This Study
	vps34Δ::KanMX4	(Lipophagy library)
ego1Δ	*(YKB4890)*	This Study
	ego1Δ::KanMX4	(Lipophagy library)
ego2Δ	*(YKB4890)*	This Study
	ego2Δ::KanMX4	(Lipophagy library)
cue4Δ	*(YKB4890)*	This Study
	cue4Δ::KanMX4	(Lipophagy library)
ubc12Δ	*(YKB4890)*	This Study
	ubc12Δ::KanMX4	(Lipophagy library)
ssb2Δ	*(YKB4890)*	This Study
	ssb2Δ::KanMX4	(Lipophagy library)
sse1Δ	*(YKB4890)*	This Study
	sse1Δ::KanMX4	(Lipophagy library)
sse2Δ	*(YKB4890)*	This Study
	sse2Δ::KanMX4	(Lipophagy library)
tgl4Δ	*(YKB4890)*	This Study
	tgl4Δ::KanMX4	(Lipophagy library)
ypr147cΔ	*(YKB4890)*	This Study
	ypr147cΔ::KanMX4	(Lipophagy library)
ypt31Δ	*(YKB4890)*	This Study
	ypt31Δ::KanMX4	(Lipophagy library)
ypt6Δ	*(YKB4890)*	This Study
	ypt6Δ::KanMX4	(Lipophagy library)
ypt11Δ	*(YKB4890)*	This Study
	ypt11Δ::KanMX4	(Lipophagy library)
hal5Δ	*(YKB4890)*	This Study
	hal5Δ::KanMX4	(Lipophagy library)
kkq8Δ	*(YKB4890)*	This Study
	kkq8Δ::KanMX4	(Lipophagy library)
npr1Δ	*(YKB4890)*	This Study
	npr1Δ::KanMX4	(Lipophagy library)
gal83Δ	*(YKB4890)*	This Study
	gal83Δ::KanMX4	(Lipophagy library)
bmh1Δ	*(YKB4890)*	This Study
(Table 3)	*bmh1Δ::KanMX4*	(Lipophagy library)
rtg1Δ	*(YKB4890)*	This Study
	rtg1Δ::KanMX4	(Lipophagy library)
vps38Δ	*(YKB4890)*	This Study
	vps38Δ::KanMX4	(Lipophagy library)
Δyvc1	*(YKB4890)*	This Study
	yvc1Δ::KanMX4	(Lipophagy library)
por2Δ	*(YKB4890)*	This Study
	por2Δ::KanMX4	(Lipophagy library)
crn1Δ	*(YKB4890)*	This Study
	crn1Δ::KanMX4	(Lipophagy library)

msl1Δ	*(YKB4890)*	This Study
	msl1Δ::KanMX4	(Lipophagy library)
hat2Δ	*(YKB4890)*	This Study
	hat2Δ::KanMX4	(Lipophagy library)
hta1Δ	*(YKB4890)*	This Study
	hta1Δ::KanMX4	(Lipophagy library)
btn2Δ	*(YKB4890)*	This Study
	btn2Δ::KanMX4	(Lipophagy library)
gvp36Δ	*(YKB4890)*	This Study
	gvp36Δ::KanMX4	(Lipophagy library)
hda1Δ	*(YKB4890)*	This Study
	hda1Δ::KanMX4	(Lipophagy library)
ubc5Δ	*(YKB4890)*	This Study
	ubc5Δ::KanMX4	(Lipophagy library)
npl4Δ	*(YKB4890)*	This Study
	npl4Δ::KanMX4	(Lipophagy library)
hsp42Δ	*(YKB4890)*	This Study
	hsp42Δ::KanMX4	(Lipophagy library)
hsp104Δ	*(YKB4890)*	This Study
	hsp104Δ::KanMX4	(Lipophagy library)
pln1Δ	*(YKB4890)*	This Study
	pln1Δ::KanMX4	(Lipophagy library)
YKB4453	***MATa*** *his3Δ1 leu2Δ0 met15Δ0 ura3Δ0 FAA4-GFP::HIS3*	GFP Collection[91]
bmh1Δ (*YKB5179*) (Figure 6)	*(YKB4453)* *bmh1Δ::KanMX4*	This Study
bmh2Δ (*YKB5180*) (Figure 6)	*(YKB4453)* *bmh2Δ::hphMX6*	This Study
hap4Δ	*(YKB4890)*	This Study
	hap4Δ::KanMX4	(Lipophagy library)
hsp26Δ	*(YKB4890)*	This Study
	hsp26Δ::KanMX4	(Lipophagy library)
hsp31Δ	*(YKB4890)*	This Study
	hsp31Δ::KanMX4	(Lipophagy library)
tfs1Δ	*(YKB4890)*	This Study
	tfs1Δ::KanMX4	(Lipophagy library)
lam6Δ	*(YKB4890)*	This Study
	lam6Δ::KanMX4	(Lipophagy library)
arv1Δ	*(YKB4890)*	This Study
	arv1Δ::KanMX4	(Lipophagy library)
atg40Δ	*(YKB4890)*	This Study
	atg40Δ::KanMX4	(Lipophagy library)
aac1Δ	*(YKB4890)*	This Study
	aac1Δ::KanMX4	(Lipophagy library)

sno4Δ	*(YKB4890)*	This Study
	sno4Δ::KanMX4	(Lipophagy library)
ubx3Δ	*(YKB4890)*	This Study
	ubx3Δ::KanMX4	(Lipophagy library)
osh1Δ	*(YKB4890)*	This Study
	osh1Δ::KanMX4	(Lipophagy library)
osh2Δ	*(YKB4890)*	This Study
	osh2Δ::KanMX4	(Lipophagy library)
osh3Δ	*(YKB4890)*	This Study
	osh3Δ::KanMX4	(Lipophagy library)
(YKB3343)	*(Y7092)*	DMA Collection
osh4Δ	*osh4Δ::KanMX4*	(GE)
osh5Δ	*(YKB4890)*	This Study
	osh5Δ::KanMX4	(Lipophagy library)
osh6Δ	*(YKB4890)*	This Study
	osh6Δ::KanMX4	(Lipophagy library)
osh7Δ	*(YKB4890)*	This Study
	osh7Δ::KanMX4	(Lipophagy library)
(YKB3900)	***MATa** his3Δ1 leu2Δ0 met15Δ0 ura3Δ0*	GFP Collection[91]
OSH1-GFP	*OSH1-GFP::HIS3*	
(YKB3901)	***MATa** his3Δ1 leu2Δ0 met15Δ0 ura3Δ0*	GFP Collection[91]
OSH2-GFP	*OSH2-GFP::HIS3*	
(YKB4255)	***MATa** his3Δ1 leu2Δ0 met15Δ0 ura3Δ0*	GFP Collection[91]
OSH3-GFP	*OSH3-GFP::HIS3*	
(YKB3264)	***MATa** his3Δ1 leu2Δ0 met15Δ0 ura3Δ0*	GFP Collection[91]
OSH4-GFP	*OSH4-GFP::HIS3*	
(YKB4257)	***MATa** his3Δ1 leu2Δ0 met15Δ0 ura3Δ0*	GFP Collection[91]
OSH5-GFP	*OSH5-GFP::HIS3*	
(YKB4256)	***MATa** his3Δ1 leu2Δ0 met15Δ0 ura3Δ0*	GFP Collection[91]
OSH6-GFP	*OSH6-GFP::HIS3*	
(YKB4258)	***MATa** his3Δ1 leu2Δ0 met15Δ0 ura3Δ0*	GFP Collection[91]
OSH7-GFP	*OSH7-GFP::HIS3*	
(YKB4932)	*(Y7092)*	This Study
ERG6-Rosella	*ERG6-Rosella::NatMX6*	
ERG6-Rosella atg8Δ	*ERG6-Rosella::NatMX6 atg8Δ::KanMX4*	This Study

Table S2. Plasmid list

Plasmid	Components	Source
PKB5	pFA6a-natMX6	Longtine *et al.* (1998)[72]
PKB6	pFA6a-kanMX4	Longtine *et al.* (1998)[72]
PKB311	pFA6a-hphMX6	Gift from Adam Rudner Lab (uOttawa)
pAS1NB cRosella I	pAS1NB-DsRed.T3-SEpHluorin	Rosado *et al.* (2008)[76]
P30416	pFA6a-GFP(S65T)-natMX6	Van Driessche *et al.* (1998)[137,138]
P44953	pFA6a-link-yomRuby2-KanMX4	Lee *et al.* (2013)[139]

Table S3. Primer list

Primer	Sequence	Description	Source
OKB2339	5'-TTCTAGCGGCTGTCAAGCCAGATGTGGAAAGAGTTTATAAAGAAAACACTCGCATCCCCCGGGTTAATTAA-3'	Forward primer for tagging *FAA4* with *GFP::NatMX6* (Used with P30416)	This work. Based on Longtine *et al.* (1998)[72] methodology
OKB2340	5'-ACGTAGTGTTTATGAAGGGCAGGGGGGAAAGTAAAAAACTATGTCTTCCTGAATTCGAGCTCGTTTAAAC-3'	Reverse primer for tagging *FAA4* with *GFP::NatMX6* (Used with P30416)	This work. Based on Longtine *et al.* (1998)[72] methodology
VPH1 tagging forward primer	5'-TATAAAGACATGGAAGTCGCTGTTGCTAGTGCAAGCCTTCCGCTTCAAGCGGTGACGGTGCTGGTTTA-3'	Forward primer for tagging *VPH1* with *mRuby2* (Used with P44953)	This work. Based on Lee *et al.* (2013)[139] methodology
VPH1 tagging reverse primer	5'-TATTTAATGAAGTACTTAAATGTTTCGCTTTTTTTAAAAGTCCTCAAAATTCGATGAATTCGAGCTCG-3'	Reverse primer for tagging *VPH1-mRuby2* with *hphMX6* (Used with PKB311)	This work. Based on Lee *et al.* (2013)[139] methodology
OKB2490	5'-TCTGTGAGGGGAGCGTTTC-3'	Reverse primer for tagging *VPH1* with *mRuby2* (Used with P44953)	This work. Based on Lee *et al.* (2013)[139] methodology
OKB2491	5'-TACGGCTCCTCGCTGCAGAC-3'	Forward primer for tagging *VPH1-mRuby2* with *hphMX6* (Used with PKB311)	This work. Based on Lee *et al.* (2013)[139] methodology

OKB2998	5'-CGCAAGCAAGTGAGAAGAAAAAGCAAGTTAAAGATAAACTAAAGATAAAACGGATCCCCGGGTTAATTAA-3'	Forward primer for *BMH1* deletion with *KanMX4* (Used with PKB6)	This work. Based on Longtine *et al.* (1998)[72] methodology
OKB2999	5'-CTTTTTTTTTTCTTTTTTTTAGTAATTTCTCTTTAGATTTATCAGAATACGAATTCGAGCTCGTTTAAAC -3'	Reverse primer for *BMH1* deletion with *KanMX4* (Used with PKB6)	This work. Based on Longtine *et al.* (1998)[72] methodology
OKB3001	5'-AAAAAGAAAAATTATCAAATCAACAAAAAGTACCCGTTACAACAAAAAAACGGATCCCCGGGTTAATTAA -3'	Forward primer for *BMH2* deletion with *hphMX6* (Used with PKB311)	This work. Based on Longtine *et al.* (1998)[72] methodology
OKB3002	5'-AGAAAACTGGAGTGGTAAATCTTCATTTCCCCTTGTATTTCTCAGCGCTCGAATTCGAGCTCGTTTAAAC -3'	Reverse primer for *BMH2* deletion with *hphMX6* (Used with PKB311)	This work. Based on Longtine *et al.* (1998)[72] methodology
OKB2501	5'-AGCCAGAAAACGCCGAAACCCCCTCCCAAACTTCCCAAGAAGCAACTCAAGGATCCCCACTAGTCGCCACCATG-3'	Forward primer for tagging *ERG6* with *Rosella* (Used with pAS1NB cRosella I)	This work. Based on Longtine *et al.* (1998)[72] methodology
OKB2504	5'-ACGAGGCAAGCTAAACAGATCTGGCGCGCCCTTAATTAACCCGGGGATCCGAACGCAGAATTTTCGAGTTATTAA-3'	Reverse primer for tagging *ERG6* with *Rosella* (Used with pAS1NB cRosella I)	This work. Based on Longtine *et al.* (1998)[72] methodology
OKB2503	5'-CGGATCCCCGGGTTAATTAAGGCGCGCCAGATCTGTTTAGCTTGCCTCGTCCCCGCCGGGTCACCCGGCCAGCG -3'	Forward primer for adding *NatMX6* onto *ERG6-Rosella* (Used with PKB5)	This work. Based on Longtine *et al.* (1998)[72] methodology
OKB2342	5'-AAATAGGTATATATCGTGCGCTTTATTTGAATCTTATTGATCTAGTGAATGAATTCGAGCTCGTTTAAAC-3'	Reverse primer for adding *NatMX6* onto *ERG6-Rosella* (Used with PKB5)	This work. Based on Longtine *et al.* (1998)[72] methodology